Progress in Oceanography
January 2022, Volume 200 Pages 102717 (13p.)
https://doi.org/10.1016/j.pocean.2021.102717
https://archimer.ifremer.fr/doc/00740/85173/

Patterns of mesozooplankton community composition and vertical fluxes in the global ocean

Soviadan Yawouvi Dodji [1, 6], Benedetti Fabio [2], Brandao Manoela C [1, 3], Ayata Sakina-Dorothée [1, 7], Irisson Jean-Olivier [1], Jamet Jean Louis [5], Kiko Rainer [1], Lombard Fabien [1, 4], Gnandi Kissao [6], Stemmann Lars [1, *]

[1] Sorbonne Université, CNRS, Laboratoire d'Océanographie de Villefranche, 06230 Villefranche-sur-mer, France
[2] Environmental Physics, Institute of Biogeochemistry and Pollutant Dynamics, ETH Zürich, Universitätstrasse 16, 8092 Zürich, Switzerland
[3] Institut Français de Recherche pour l'Exploitation de la Mer, Centre Bretagne, 29280 Plouzané, France
[4] Institut Universitaire de France (IUF), Paris, France
[5] Université de Toulon, Mediterranean Institute of Oceanology (MIO), AMU-UTLN UM110, Equipe EMBIO, CS 60584, 83041 TOULON Cedex 9, France
[6] Département de Géologie, Université de Lomé, Togo
[7] Sorbonne Université, CNRS, IRD, MNHN, Laboratoire d'Océanographie et du Climat: Expérimentations et Approches Numériques (LOCEAN-IPSL), Paris, France

* Corresponding author : Lars Stemmann, email address : stemmann@obs-vlfr.fr

Abstract :

Vertical variations in physical and chemical conditions drive changes in marine zooplankton community composition. In turn, zooplankton communities play a critical role in regulating the transfer of organic matter produced in the surface ocean to deeper layers. Yet, the links between zooplankton community composition and the strength of vertical fluxes of particles remain elusive, especially on a global scale. Here, we provide a comprehensive analysis of variations in zooplankton community composition and vertical particle flux in the upper kilometer of the global ocean. Zooplankton samples were collected across five depth layers and vertical particle fluxes were assessed using continuous profiles of the Underwater Vision Profiler (UVP5) at 57 stations covering seven ocean basins. Zooplankton samples were analysed using a Zooscan and individual organisms were classified into 19 groups for the quantitative analyses. Zooplankton abundance, biomass and vertical particle flux decreased from the surface to 1000 m depth at all latitudes. The zooplankton abundance decrease rate was stronger at sites characterised by oxygen minima (<5µmol O2.kg−1) where most zooplankton groups showed a marked decline in abundance, except the jellyfishes, molluscs, annelids, large protists and a few copepod families. The attenuation rate of vertical particle fluxes was weaker at such oxygen-depleted sites. Canonical redundancy analyses showed that the epipelagic zooplankton community composition depended on the temperature, on the phytoplankton size distribution and the surface large particulate organic matter while oxygen was an additional important factor for structuring zooplankton in the mesopelagic. Our results further suggest that future changes in surface phytoplankton size and taxa composition and mesopelagic oxygen loss might lead to profound shift in zooplankton abundance and community structure in both the euphotic and

mesopelagic ocean. These changes may affect the vertical export and hereby the strength of the biological carbon pump.

Highlights

► A comprehensive analysis of variations in zooplankton community composition and vertical particle flux in the upper kilometer of the global ocean. ► Epipelagic zooplankton community composition depends on the temperature, on the phytoplankton size distribution and the surface large particulate organic matter. ► Oxygen was an additional important factor for structuring zooplankton in the mesopelagic. ► Low vertical attenuation of zooplankton abundance and biomass goes in hand with high particle flux attenuation and vice versa.

Keywords : Zooplankton, Biological carbon pump, Epipelagic, Mesopelagic, Community structure, Particle flux, Attenuation rates, Oxygen, Minimum Zone

Introduction

The upper kilometer of the ocean constitutes a habitat where most of the organic carbon produced by the phytoplankton in the epipelagic layer (0-200m) sinks into the mesopelagic layer (200-1000m) while being progressively consumed and respired. Within the wide size spectrum of planktonic organisms (0.02µm-2m), mesozooplankton (0.2-20mm) are a pivotal component of marine trophic webs impacting the Biological Carbon Pump (BCP) through their feeding, vertical migration, and the production of faecal pellets (Steinberg and Landry, 2017). In a context of global climate change, zooplankton communities experience increasingly stressful conditions through global warming, ocean acidification and deoxygenation (Oschlies et al., 2018; Schmidtko et al., 2017), enhanced water column stratification in the open ocean and modifications in phytoplankton production and community structure (Coma et al., 2009; Kwiatkowski et al., 2019; Richardson, 2008). Long term field surveys have shown how shifts in climatic conditions lead to large shifts in surface zooplankton composition (Beaugrand et al., 2019). Future climate warming could further reduce macronutrient supplies in the upper ocean and therefore decrease phytoplankton biomass in the tropical open ocean or can cause positive trophic amplification in the polar ocean (Chust et al., 2014). Such changes in biomass may be amplified in the zooplankton through trophodynamic effects, which could greatly alter the fluxes of organic matter into the deeper mesopelagic layers. Within the latter, modifications of the quantity and quality of the vertical particle flux produced in the surface layers could trigger substantial changes in mesozooplankton abundance and composition. In addition, the expansion of Oxygen Minimum Zones (OMZ) (Schmidtko et al., 2017; Stramma et al., 2010) may further constrain the spatial distribution of the numerous zooplankton taxa that are sensitive to dissolved oxygen levels (Ekau et al., 2010; Kiko et al., 2020; Kiko and Hauss, 2019; Seibel, 2011; Wishner et al., 2020, 2018). Therefore, understanding the variations of zooplankton biomass and diversity in the epi and mesopelagic is essential to better understand the impact of global climate change on the properties of marine ecosystems.

However, mesopelagic zooplankton communities remain critically under-sampled compared to the epipelagic ones, as most collections is in the first 200m of the water column (Everett et al., 2017). The mesopelagic is still considered a “dark hole” (Robinson et al., 2010; St John et al., 2016) as the gaps in sampling lead to critical gaps in knowledge regarding the functioning of mesopelagic ecosystems and how they are controlled by the organic matter fluxing from the euphotic zone. Local to regional field studies reported that the abundance of mesozooplankton decreases exponentially with depth, in parallel with substantial changes in species diversity and genus composition that remain poorly resolved (Bode et al., 2018;

Brugnano et al., 2012; Hernández-León et al., 2020; Koppelmann et al., 2005; Kosobokova and Hopcroft, 2010; Yamaguchi et al., 2004). Some studies reported increases in diversity with depth, with maxima in the meso- to bathypelagic layers (Bode et al., 2018; Gaard et al., 2008; Kosobokova and Hopcroft, 2010; Yamaguchi et al., 2004), whereas other studies reported either the opposite diversity pattern or even an absence of vertical patterns due to large spatio-temporal variability (Gaard et al., 2008; Hidalgo et al., 2012; Palomares-García et al., 2013; Wishner et al., 2008). Such mismatch between observations might be related to the wide range of environmental conditions sampled using a variety of sampling gears that make inter-comparisons difficult. One recent global analysis of zooplankton vertical distribution in inter-tropical regions showed that in this narrow latitudinal band the vertical dimension was the main structuring pattern suggesting that midwater processes mediated by zooplankton may not change between oceans at those latitudes (Fernández de Puelles et al., 2019). How these changes relate to the vertical flux and also across the full latitudinal band is poorly understood because plankton observations and biogeochemical studies have usually been carried out by distinct scientific communities. Recent interdisciplinary cruises have taken place, providing more integrated knowledge on the importance of zooplankton to carbon sequestration (Guidi et al., 2016; Kiko et al., 2020; Steinberg and Landry, 2017; Stukel et al., 2019). No global study has yet been able to analyse community-level variations in zooplankton abundances, biomass and community composition in conjunction with assessments of vertical particle flux in the upper kilometre of the global ocean.

Here, a homogeneous dataset of community-level zooplankton images generated from the TARA Oceans expeditions is explored together with associated measurements of their contextual environmental conditions to: (i) test whether zooplankton communities present consistent vertical variations in abundance and composition across the oceans and in different latitudinal bands, and (ii) investigate the main drivers of such vertical gradients and how they are coupled to the surface phytoplankton and estimates of particle flux. The TARA Oceans expedition collected over 35000 samples encompassing the whole plankton community (i.e., from viruses to jellyfish) across the global ocean from 2009 to 2013 (Karsenti et al., 2011). Previous studies that analysed the TARA Oceans imaging dataset explored the global latitudinal gradients in richness and composition for the whole plankton community focusing on surface waters (Ibarbalz et al., 2019; Brandao et al., in press). Here, we aim to describe the community composition of mesozooplankton down to 1000m depth on a global scale. As the imaging techniques used here cannot achieve a species-level identification of the zooplankton

community composition, our approach is rather oriented towards larger taxonomic and /or functional groups that may be associated with broad ecological and biogeochemical functions.

Materials and methods

Sampling sites and environmental variables

TARA Oceans took place between 2009 and 2013. Among the 210 stations that were sampled, 57 stations covering 7 ocean basins (Fig. 1) were sampled with a Multinet (Pesant et al., 2015; Roullier et al., 2014), a sampling device with five nets that allows for depth-stratified sampling (see below).

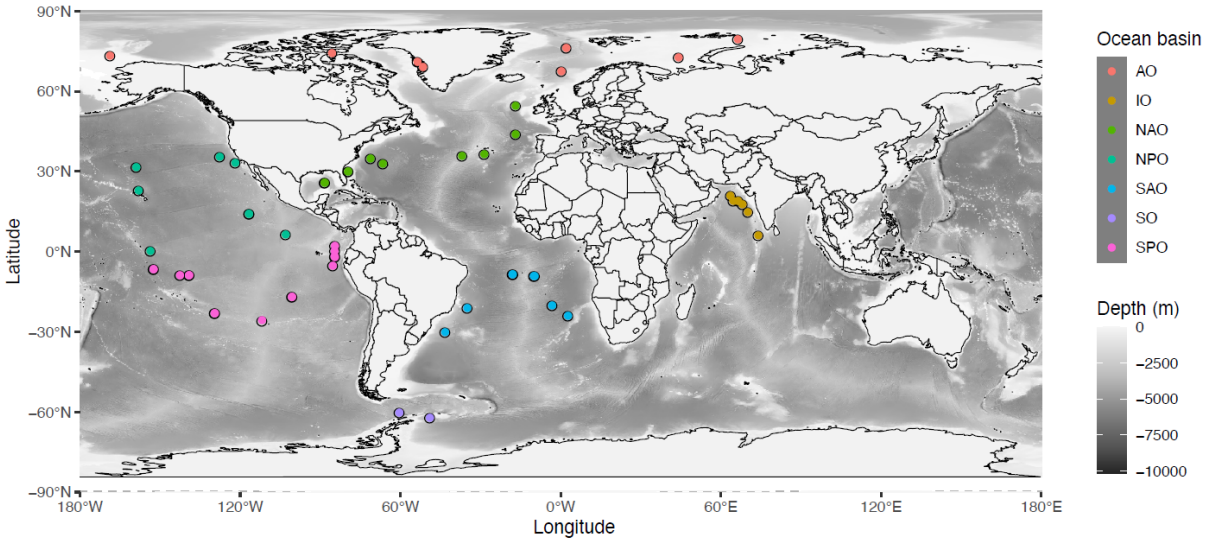

Fig. 1: Location of the 57 stations sampled with the Multinet, grouped by ocean basin: AO=Arctic Ocean, IO=Indian Ocean, NAO=North Atlantic Ocean, NPO=North Pacific Ocean, SAO=South Atlantic Ocean, SO=Southern Ocean or Austral Ocean, SPO=South Pacific Ocean.

A CTD rosette equipped with optical sensors was deployed to measure the physico-chemical parameters within the water column. Temperature and conductivity were measured from the surface to a maximum of 1300 m depth using a Seabird 911 CTD mounted on a Sea-Bird Carousel sampler with 10 Niskin bottles. The following additional sensors were mounted to measure optical properties related to relevant biogeochemical variables: fluorometer (Wetlab ECO-AFL/FL model), dissolved oxygen sensor (model SBE 43), nitrate sensor (ISUS with a maximum rating depth of 1000m Satlantic SA), a 25 cm transmissometer for particles 0.5–20 µm (WETLabs), a one-wavelength backscatter meter for particles 0.5–10 µm (WETLabs), and an Underwater Vision Profiler 5 (UVP5) for particles >150 µm and zooplankton >600 µm

(Hydroptic). Assuming that particle sinking speed increases with size, those particles detected through the backscattering will be referred to as suspended particulate matter (SPM, particles < 10µm in Equivalent Spherical Diameter), while the ones detected by the UVP5 (>150µm in Equivalent Spherical Diameter) will be referred as particles. Vertical particle mass flux (in mg Dry Weight $m^{-2}d^{-1}$)) was calculated from the particle size spectra detected by the UVP5 as in (Guidi et al., 2008). Based on the High Pressure Liquid Chromatography (HPLC) analysis of water collected with Niskin bottles, we used the method of Uitz et al. (2006) to estimate the contribution (%) of three pigment size classes (microphytoplankton, nanophytoplankton, and picophytoplankton; f_micro, f_nano, and f_pico, respectively) to total phytoplankton biomass in the epipelagic layer. The median value of all hydrological and optical data together with imaging data were calculated for each of the five horizontal layers sampled by the Multinet for future data processing. The samples were classified as anoxic, hypoxic and normoxic according to the oxygen minimum value measured within the towed layer. We used a threshold of 5 $\mu mol\ kg^{-1}$ to classify the stations as anoxic (Roullier et al., 2014) and 58.5 $\mu mol\ kg^{-1}$(Bode et al., 2018) to classify them as hypoxic.

Zooplankton sampling, digitization, biomass estimates

A Hydrobios Multinet (with a 300µm mesh and an aperture of $0.25m^2$) was used to sample zooplankton (Roullier et al., 2014; Pesant et al., 2015) in five distinct water layers ranging from the surface to occasionally 1300 m depth. The five depth layers were locally defined as a function of the vertical structure of the water column according to the profiles of temperature, salinity, fluorescence, nutrients, oxygen, and particulate matter (Pesant et al., 2015). The Multinet was equipped with a flowmeter to measure the volume of seawater filtered by each net tow (Pesant et al., 2015). Day and night net tows were conducted at ten stations. Sampling at the other stations occurred at day or night, depending on cruise schedule and operational constraints. Once collected, the samples were preserved in a solution of buffered formaldehyde-Borax solution (4%). In the laboratory, the samples were rinsed and split with a Motoda box (MOTODA, 1959). The final split was analysed with the Zooscan imaging system (Gorsky et al., 2010) which allowed a rapid and semi-automatic analysis of zooplankton samples. In total, the samples comprised nearly 400,000 images of living zooplankton and detritus. These images were imported into Ecotaxa, an online platform which allows an automatic prediction of the taxonomic classification of each single image followed by a manual validation/correction. The organisms were then identified manually down to the order, sometimes to the family and rarely down to the genus level. All copepods were sorted at the

family level apart from the smallest copepods that cannot be recognised at the family level from the image. They were all grouped into one category called Other-copepoda or other-Calanoida if their morphological features allowed classifying them as Calanoida. This initial sorting allowed classifying zooplankton into 119 taxa. As many taxa showed a very small contribution to total zooplankton abundance, the 119 taxa were grouped into 19 taxonomic groups (Table 1). Those include all the major zooplankton groups that are frequently observed in the oceans. To investigate vertical patterns in mesozooplankton abundance, these 19 groups were further aggregated into eight groups representing a combination of taxonomic and functional classification (Table 1).

Once the zooplankton images were sorted, Ecotaxa enabled us to extract the concentration and the biovolume of each mesozooplankton group at every station and for every net tow, while accounting for the Motoda fraction and the volume sampled. The biovolume was computed for each individual zooplankton using the minor and major length axes assuming a prolate ellipsoidal shape (Gorsky et al., 2010). The biomass was calculated for the 8 large groups using the equations for the different taxa :

$$Body\ Weight(\mu C) = aS^b \quad (1)$$

where S is body area in mm^2. Taxon-specific area-to-dry mass conversion factors (Lehette and Hernandez-Leon, 2009) and dry mass to carbon (C) conversion factors (Kiørboe, 2013) were used to calculate the biomass and C content of each zooplankton organism scanned. Taxonomic units and biomass conversion factors used are listed in Table 2. For large protists the conversion factor was adjusted to $0.08\ mgC\ mm^{-3}$ (Biard et al., 2016).

Shannon diversity index (H') was calculated based on the relative abundances of the 119 taxa for each sample as follows:

$$H' = -\sum_i^n \quad p_i log p_i \quad (2)$$

where p_i is relative abundance of each taxa in one sample and log is the natural logarithm.

Analyzing zooplankton and particles vertical distributions

Vertical attenuation rates of zooplankton (abundance and biomass) and estimated particle fluxes were estimated, from the five sampled layers for zooplankton and from the 5 meter resolution profile of estimated vertical flux using a linear regression of the log-log (i.e. natural logarithm) with the following equation :

$$X = X_0(Z/Z_0)^b \quad (3)$$

where X represents the zooplankton abundance, the zooplankton biomass or the particle vertical flux at the depth level Z, X_0 the zooplankton biomass or abundance and vertical particle flux at the depth Z_0 (chosen as median depth of the surface net) and b the slope taken as a proxy of the attenuation rate of zooplankton biomass zooplankton abundance or particle flux. In the rest of the manuscript, A_zoo represents the slope b of vertical profile for zooplankton abundance, B_zoo the slope b of vertical profile for zooplankton biomass, A_flux the slope b of vertical profile for particle flux, and P_flux1, P_flux2 and P_flux3 the particle flux in respectively the epipelagic, upper and lower mesopelagic. To analyse latitudinal patterns in attenuation rates, the slope values were separated into three latitudinal bands based on the latitudinal position of their corresponding sampling stations: intertropical (0°-30°), temperate (30-60°) and polar (60°-90°). The intertropical stations gathered both OMZ and non-OMZ stations, which allowed us to analyse the effect of oxygen depletion on zooplankton and particles. Non-parametric variance analyses (Kruskal and Wallis tests) were performed to test for differences in slope values (i.e. zooplankton and particles attenuation rates) between latitudinal bands.

Multivariate analysis of community composition

To explore the response of zooplankton community composition to environmental drivers across depth layers, the non-interpolated abundances of the 19 taxonomic groups mentioned above were aggregated into three layers: the epipelagic layer (0-200m), the upper mesopelagic layer (200-500m) and the lower mesopelagic layer (500-1000m). To analyse separately the three depth layers, the samples collected in overlapping layers (18.59% of the total samples) were not included in the statistical analysis (Table S1). To characterise the environmental conditions of each layer at each sampling station the median values of the following contextual environmental variables were used: temperature (T), salinity (S), oxygen (O_2), nitrate concentration (NO_3), chlorophyll *a* concentration (Chl_*a*), phytoplankton size fractions ($f_{\_micro}$, $f_{\_nano}$, and $f_{\_pico}$), concentration of suspended particles (SPM) and particle flux (P_Flux). The measurements of all these environmental variables are available on PANGAEA (https://doi.org/10.1594/PANGAEA.840721).

To estimate the strength of the Diel Vertical Migration (DVM) at 10 stations, pairwise Wilcoxon tests were performed to compare in each layers the abundance and biomass of each taxa between day and night. For those 10 same pairs of stations, we used an analysis of similarities (ANOSIM) to test for significant variations in community composition between day and night samples. The ANOSIM tested whether the inter-groups difference (day and night

groups) was higher than the intra-groups difference, by providing an R coefficient. An R coefficient close to one suggests dissimilarity between groups, while R value close to zero suggests an even distribution of high and low ranks within and between groups. An R value below zero suggests that dissimilarities are greater within groups than between groups (Clarke and Gorley, 2001). ANOSIM tests were performed within each layer using log-transformed (where log is the natural logarithm) abundances and Bray-Curtis distance among stations.

For each depth layer, a canonical redundancy analysis (RDA) was performed based on the abundances of the 19 mesozooplankton groups and the above-mentioned environmental variables to explore the explanatory power of these variables in structuring the mesozooplankton community. The RDA is an extension of the multiple regression analysis applied to multivariate data (Legendre and Legendre, 1998). It allows representing the response variables (abundances of the 19 mesozooplankton groups) in a "constrained" reduced space, i.e., constructed from the explanatory variables (the environmental variables). For each RDA, the following variables were used as "supplementary variables" of the analysis in order to visualize their correlation with the environmental structuring of the mesozooplankton community (i.e., to visualise their position in the RDA space): attenuation of particle flux (A_flux), attenuation of zooplankton abundance (A_zoo), attenuation of zooplankton biomass (B_zoo) and the Shannon index (*H'*). Beforehand, a Hellinger transformation was performed on the mesozooplankton abundances. A preliminary RDA based on all samples together showed a very strong effect of depth on mesozooplankton community composition (Fig. S1). Therefore, to avoid such a strong effect of depth on the community composition analysis, three separate RDAs were performed on each of the three layers defined above. Significant axes were identified using the Kaiser-Guttman criterion (Legendre and Legendre, 1998).

Data manipulation and statistical analyses were performed with Matlab 2018b (MATLAB 9.5) for the vertical profiles of abundance and biomass and statistical test (Wilcoxon test, Kruskal-wallis test), R environment v3.5.1 (using the following packages: vegan version 2.5-5, ggplot2 version 3.1.1, ggrepel version 0.8.0 and ggfortify version 0.4.7) for the redundancy analysis and PRIMER6 (Version 6.1.12) and PERMANOVA+ (Version 1.0.2) for the ANOSIM test.

Results

Day night variability

In each layer, the comparison between day/night of the taxonomic groups indicated that only a few groups (Euphausiidae, Metridinidae, Corycaeidae and Cnidaria for abundance; Eumalacostraca and Ostracoda for biomass) showed significant differences in either the surface layer or the upper mesopelagic layer (Table S1). Nonetheless, the ANOSIM found no significant differences in the community composition between the day and night samples at the community-level (R0-200m = -0.039; R200-500m = -0.008; R500-1100m = -0.006). The same analyses based on biomass also indicated no significant differences (R0-200m = 0.018; R200-500m = -0.051; R500-1100m = 0.087). As a consequence, all further analyses were carried out without making any distinctions between day and night samples.

Vertical patterns in zooplankton total abundance and biomass and particle flux

On a global scale, zooplankton abundance and biomass decreased exponentially with depth (Fig. 2) in the different latitudinal bins. Abundance and biomass decrease rate with depth and were correlated ($r2=0.342$, $p=4.6\ 10^{-5}$) but the biomass attenuation rate estimates were systematically lower than the attenuation based on the abundance profiles. On average, polar waters showed increased zooplankton abundance and biomass compared to the stations located in the tropics. In the epipelagic layer, abundances and biomass ranged from 1 to 5000 ind m^{-3} and 0.05 to 200 mg C m^{-3} while in the mesopelagic they were reduced to 0.05 to 450 ind m^{-3} and 0.005 to 40 mg C m^{-3}. Copepods were the most abundant being 85% and 65% of the abundance and biomass in the epipelagic, 85 and 76% in the upper mesopelagic and 95% and 97% in the lower pelagic (Table 3). The estimated vertical flux also decreased with depth in all latitudinal bands. On average polar waters showed higher fluxes compared to the stations located in the tropics.

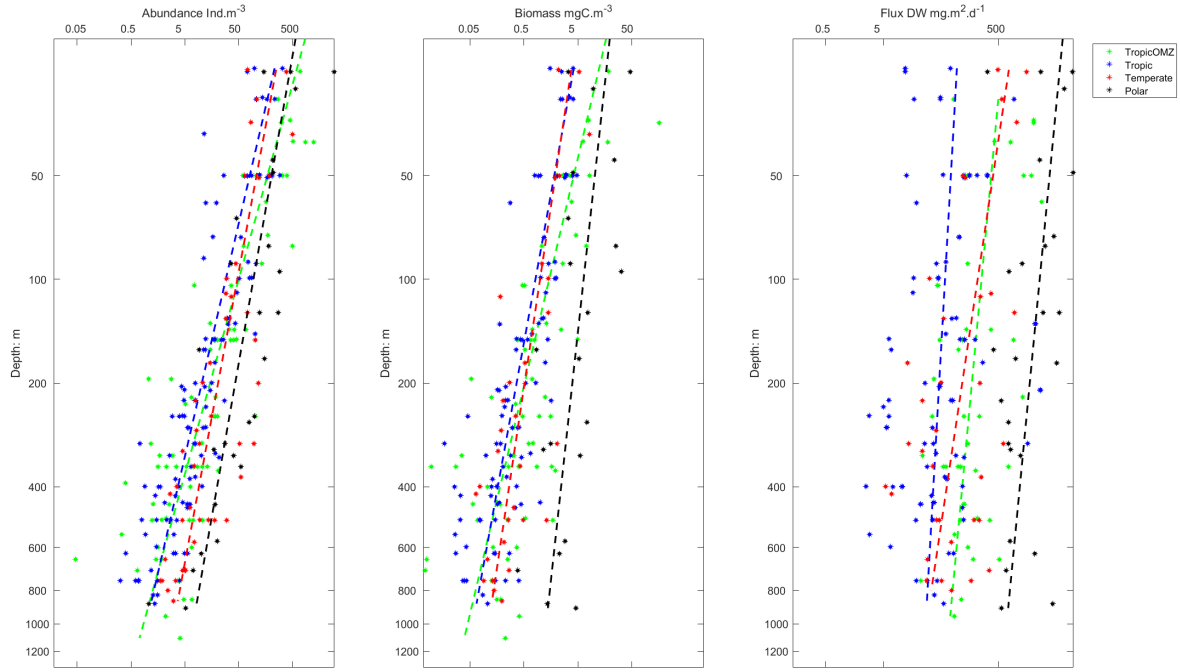

Fig. 2: Vertical distribution of zooplankton biomass, abundance and particle flux in different latitudinal bands. Dotted lines represent the fitted linear regression for each latitudinal band (equation 3). The linear fits to the data point are given in table 4.

The attenuation rates of zooplankton abundance and biomass with depth were stronger than the attenuation rates of the vertical particle flux (Fig. 3A, B and C, Table 4). The decrease rates in zooplankton vertical abundance and biomass are more pronounced in OMZ stations compared to the non-OMZ stations. Yet, such difference was found to be significant only when the vertical decrease rates were calculated from abundances. In general, zooplankton attenuation rates decreased with latitude whereas the attenuation rates of particle fluxes increased with latitude (Fig. 3, Table 3). A non-parametric variance analysis (Kruskal-Wallis test) of the attenuation rate revealed significant differences in the attenuation rates of zooplankton abundances between the anoxic tropical stations and the temperate and polar ones, but not with the other tropical stations (Table 4). No statistical difference between regions was found. The attenuation rate of vertical flux was weaker at the OMZ sites compared to the non OMZ ones but this difference was not significant (Fig. 3B).

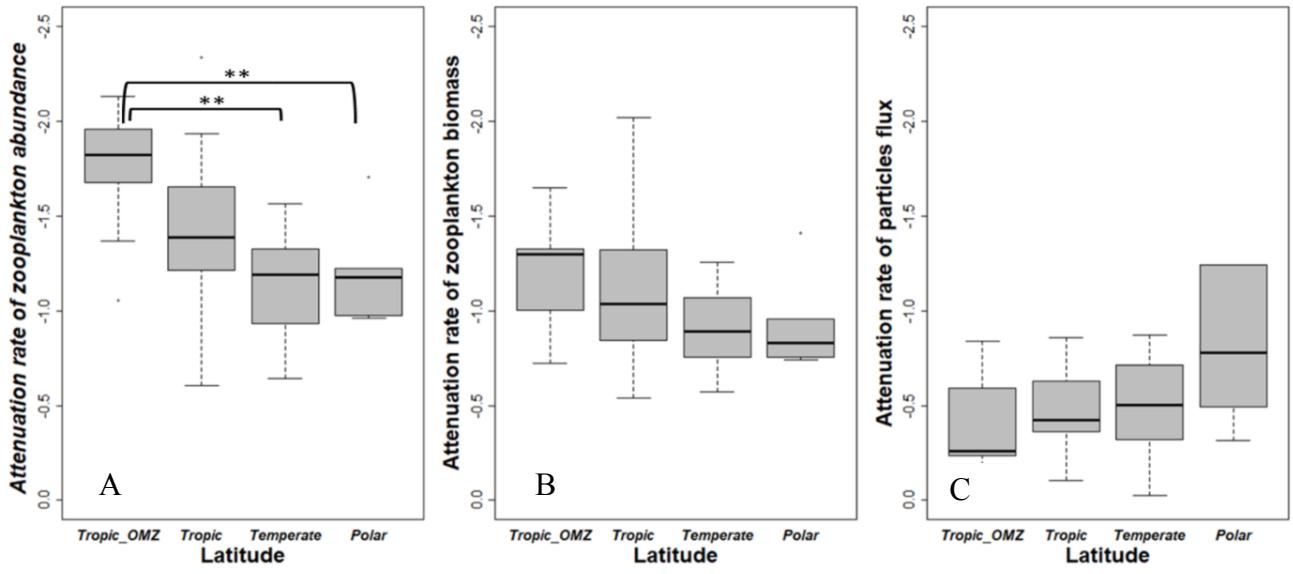

Fig. 3: Distributions of attenuation rates at each station per latitudinal bands (Tropical, Tropical OMZ, Temperate, and Polar). A: Attenuation rate of zooplankton abundance (A_zoo). B: Attenuation rate of zooplankton biomass (B_zoo). C: Attenuation rate of particle flux (A_flux). (**) means significant Kruskal-Wallis test with $p < 0.01$ (Table 5).

Structuring of the epipelagic community composition.

In the epipelagic layer (0 – 200 m depth), the environmental variables explained 32.71% of the total variance in mesozooplankton groups' abundances. The first RDA axis (RDA1, 57.18 % of constrained variance) opposed the samples from polar waters, and especially those from the Arctic dominated by Calanidae and crustacean larvae (RDA1 > 0), to the tropical samples presenting more even contributions from most of the remaining groups: Protista, Eumalacostraca, Annelida, Amphipoda, Corycaeidae, Chaetognatha, Euphausiacea, Oithonidae, Ostracoda, Oncaeidae, Calanoida (RDA1 < 0). RDA1 was negatively scored by temperature and salinity and positively scored by vertical particle flux, microphytoplankton contribution, suspended particle concentration, dissolved oxygen concentration and chlorophyll *a* concentration. Among the supplementary variables, the attenuations of the particle flux and of the zooplankton biomass were positively correlated with RDA1, while the attenuation of the zooplankton abundance and the Shannon index were negatively correlated to RDA1. RDA2 (13.1% of constrained variance) opposed the samples from the Indian Ocean and North Atlantic Ocean that present higher abundances of Cnidaria, Mollusca, Tunicata and Cladocera (RDA2 < 0) to those samples from the Southern Ocean presenting higher abundances of Annelida, Euphausiacae, Amphipoda and Other Copepoda (RDA2 > 0). RDA2 was positively scored by

nitrate concentrations and the relative contribution of nanophytoplankton. It was negatively scored by the concentration of suspended particles and the relative contribution of microphytoplankton. All supplementary variables were negatively correlated with RDA2.

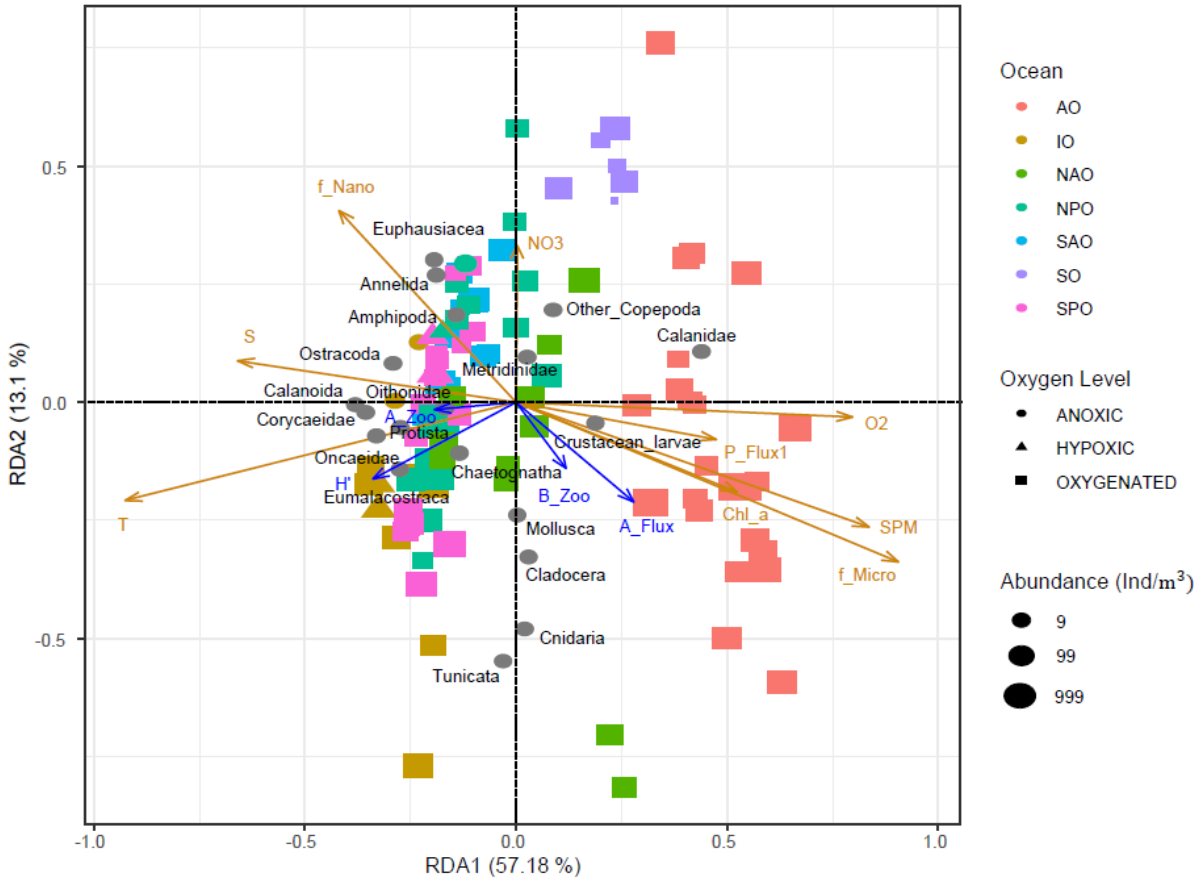

Fig. 4: RDA on the epipelagic communities. Each dot corresponds to a sample, i.e., one net at one depth at one station. The orange arrows correspond to the quantitative environmental variables in RDA space: f_pico, f_nano and f_micro correspond to the relative contribution (%) of pico-, nano- and micro-phytoplankton to total phytoplankton biomass, O2 = dissolved oxygen concentration (µmol/kg), Chl_a = Chlorophyll a concentration (mg/m3), SPM = suspended particles matter (m/sr), T = temperature (°C), Sal = salinity, NO3 = nitrate concentration (mol/kg), Z = depth (m)) and P_Flux= particulate flux ($mg.m^{-2}.d^{-1}$). Grey dots mark the projection of the zooplankton groups abundance ($ind.m^{-3}$). Colors correspond to the ocean basin where the samples were taken: AO = Arctic Ocean, IO = Indian Ocean, NAO = North Atlantic Ocean, NPO = North Pacific Ocean, SAO = South Atlantic Ocean, SO = Southern Ocean, SPO = South Pacific Ocean. Shapes illustrate oxygen level, Anoxic: [O_2] <5µmol/kg; Hypoxic: 5µmol/kg< [O_2] <58.5µmol/kg and oxygenated: [O_2]>58.5µmol/k). Supplementary variables estimated for the epipelagic layer are represented with blue arrows: attenuation of particle flux (A_flux), attenuation of zooplankton abundance (A_zoo), attenuation of zooplankton biomass (B_zoo) and the Shannon index (*H'*).

Structuring of the upper mesopelagic community composition.

In the upper mesopelagic layer (200 to 500 m depth), the environmental variables explained 29% of the total variance in mesozooplankton groups' abundances. Again, the first RDA axis (RDA1, 36.33% of constrained variance) mainly opposed the polar samples dominated by Calanidae copepods, and characterized by higher concentrations of suspended particle, particle flux (both from surface and upper mesopelagic layer), and higher dissolved oxygen concentrations (RDA1 > 0), from the samples characterized by more diverse zooplankton communities (mainly Corycaeidae, small Calanoida, Oncaeidae) and correlated to higher temperature, higher salinity and a higher relative contribution of the nanophytoplankton (RDA1 < 0). Similarly, to what was observed for the epipelagic layer, among the supplementary variables, the attenuations of the particle flux and of zooplankton biomass were positively correlated with RDA1, while the attenuation of zooplankton abundance and the Shannon index were negatively correlated to RDA1. RDA2 (24.72% of constrained variance) opposed the anoxic samples from the Indian Ocean presenting higher abundances of Tunicata, Annelida, Protista, Mollusca, Oithonidae and Cnidaria (RDA2 < 0) to the oxygenated ones displaying higher abundances of Ostracoda, Eumalacostraca, crustacean larvae, other Copepoda, Chaetognatha and Euphausiacea (RDA2 > 0). Samples from the Arctic Ocean were dominated by large copepods from the Calanidae and Metridinidae families. Samples from the Pacific and Atlantic Oceans were dominated by other Copepoda, Eumalacostraca, Ostracoda, Euphausiacea, Chaetognatha and crustacean larvae. Higher attenuation rates of zooplankton biomass and particle flux were found in polar samples whereas higher zooplankton attenuation rates were found in warmer waters, especially at OMZ stations. Again, samples from the tropical upper mesopelagic layers displayed more diverse communities. The distribution of the supplementary variables along RDA2 differed from what was observed for the epipelagic layer, as the supplementary variables, except the attenuation of the zooplankton abundances, were positively correlated to RDA2.

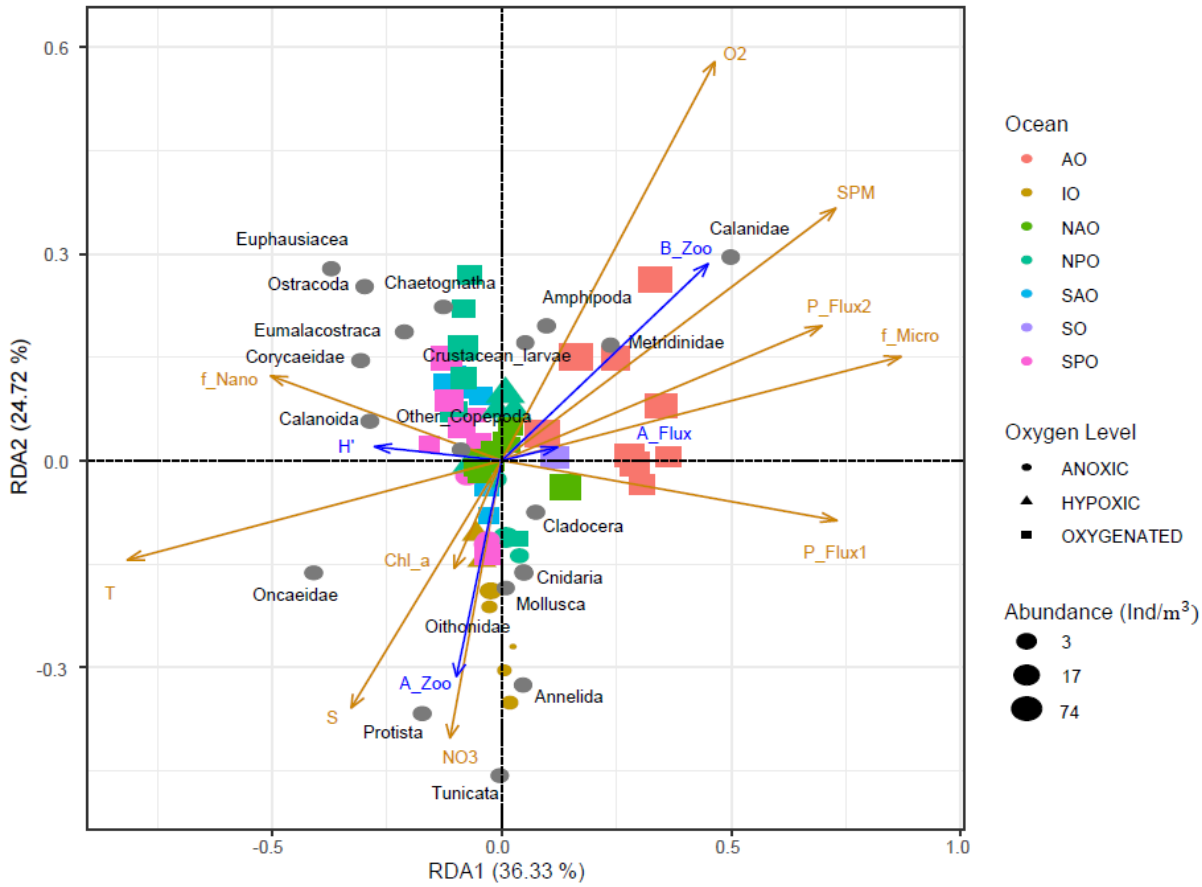

Fig. 5: RDA performed on the upper mesopelagic abundances. Each dot corresponds to a sample, i.e., one net at one depth at one station. The orange arrows correspond to the quantitative environmental variables (see legend of Fig. 4). Anoxic: $[O_2]$ <5µmol/kg; Hypoxic: 5µmol/kg< $[O_2]$ <58.5µmol/kg and oxygenated: $[O_2]$>58.5µmol/kg). Supplementary variables estimated for the upper mesopelagic layer are represented with blue arrows: attenuation of particle flux (A_flux), attenuation of zooplankton abundance (A_zoo), attenuation of zooplankton biomass (B_zoo) and the Shannon index (*H'*).

Structuring of the lower mesopelagic community composition

In the lower mesopelagic layers (500 to 1000 m depth), the environmental variables explained 29.46 % of the total variance in mesozooplankton groups' abundances. The first RDA axis (RDA1, 35.14 % of constrained variance) opposed the stations from the Arctic and North Atlantic Oceans characterized by higher dissolved oxygen concentrations, higher suspended particle concentrations (RDA1 > 0), from the anoxic and nitrate-rich stations from the Indian Ocean (RDA1 < 0). The former stations were characterized by higher abundances of Calanidae, Calanoida, Metridinidae, crustacean larvae, Ostracoda and Amphipoda, whereas the latter were characterized by higher abundances of Tunicata, Annelida, Eumalacostraca and other Copepoda. RDA2 (22.08 % of constrained variance) separated the colder and less salty stations of the Southern Atlantic Ocean (RDA2 < 0) from the warmer, saltier stations (RDA2 > 0) of

the North Atlantic and the Indian Oceans that are characterized by less diverse zooplankton communities. The stations that sampled the oxygenated waters of the North Atlantic and Arctic Oceans were dominated by large copepods of the Metridinidae and Calanidae families, as well as most of the small other Calanoida (i.e. those smaller copepods that could not recognized at a more detailed taxonomic level) in addition to Ostracoda, Amphipoda, and crustacean larvae. Oxygenated stations from the South Atlantic Ocean (SAO) were characterized by higher abundances of Chaetognatha, Corycaeidae, Euphausiacea, Cnidaria, Mollusca, Oithonidae, Oncaeidae and Protista. Samples taken in the OMZ of the Indian and North Pacific Oceans displayed higher abundances of other Copepoda, Tunicata, Annelida, Eumalacostraca and Protista. Higher mesozooplankton biomass and stronger particle flux attenuation rates were found in the normoxic waters while higher zooplankton attenuation rates were observed at the stations that sampled an OMZ. The distribution of the supplementary variables showed similar association with environmental variables as in the upper mesopelagic.

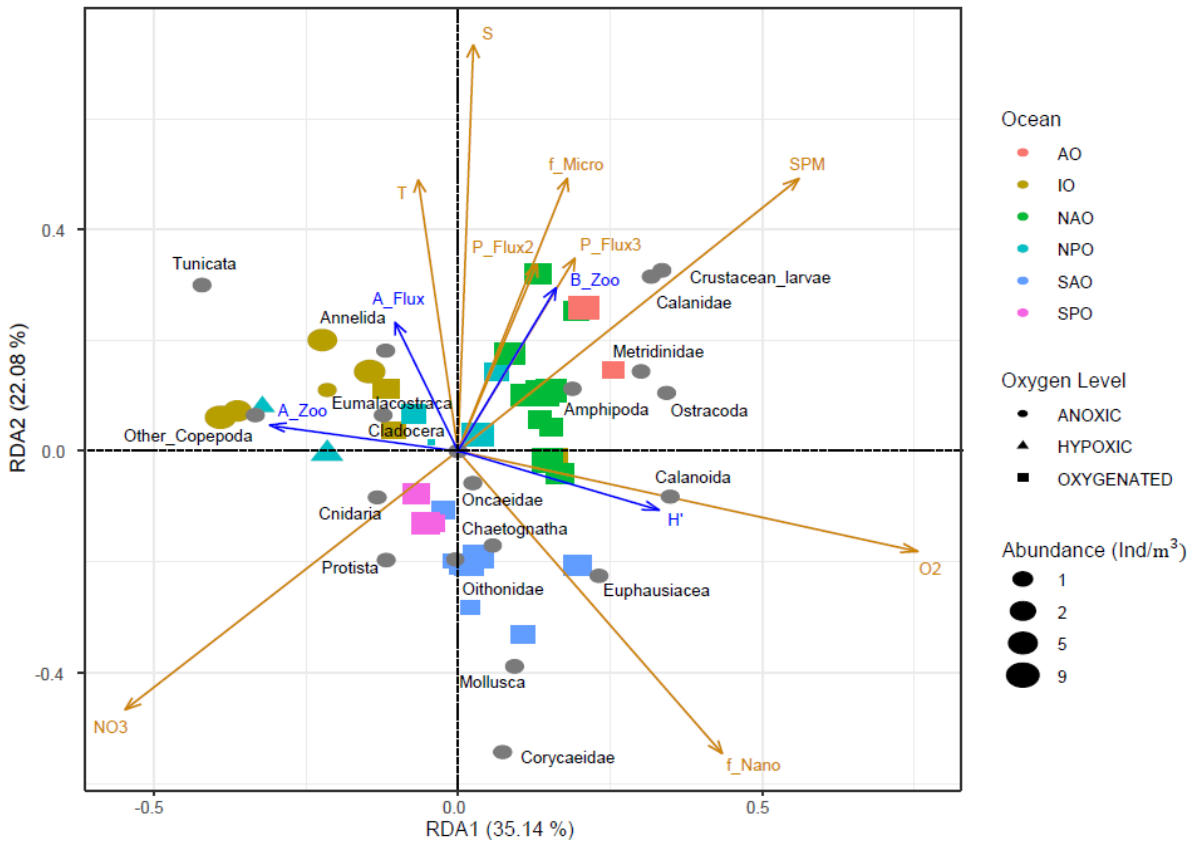

Fig. 6: RDA performed on the lower mesopelagic abundances. Each dot corresponds to a sample, i.e., one net at one depth at one station. The orange arrows correspond to the quantitative environmental variables (see legend of Fig. 4). Anoxic: $[O_2]$ <5µmol/kg; Hypoxic: 5µmol/kg< $[O_2]$ <58.5µmol/kg and oxygenated: $[O_2]$>58.5µmol/kg). Supplementary variables estimated for the lower mesopelagic layer

are represented with blue arrows: attenuation of particle flux (A_flux), attenuation of zooplankton abundance (A_zoo), attenuation of zooplankton biomass (B_zoo) and the Shannon index (*H'*).

Discussion

The present global analysis of spatial patterns of the mesozooplankton community and their relationship with the strength of the vertical particle flux is based on zooplankton abundance and biomass estimates and vertical particles flux estimated using state-of-the-art imaging techniques (Zooscan and UVP5). The rigorous quality control (see Supplementary Material) allows to depict with confidence correlations between zooplankton and particle flux, two important components of the biological carbon pump (BCP). Notably the study allows to infer global ecological patterns in the epipelagic and mesopelagic layers, the coupling between these two layers in oxygenated, hypoxic and anoxic situations.

Important environmental factors for the mesozooplankton community composition in the epipelagic layer

High latitude marine ecosystems are characterised by a combination of lower species diversity and shorter food webs (Laws, 1985; Stempniewicz et al., 2007) sustained by higher concentrations of large microphytoplankton cells (diatoms). On the contrary, low latitude ecosystems are featured by more complex and diverse food webs (Saporiti et al., 2015; Uitz et al., 2006) adapted to lower production rates ensured by smaller cells (i.e. pico- and nanoplankton). How the dynamics of zooplankton community composition and vertical particle flux follow this scheme remains more elusive. Previous field-based studies reported peaks in zooplankton species richness in the tropics (Rombouts et al., 2010; Rutherford et al., 1999; Yasuhara et al., 2012), which is in line with the above-mentioned theory that the tropical food-depleted regions promote more complex food-webs with higher species richness. Our RDAs results result supports the view that, on a global scale, temperature and the production regime of surface ecosystems are the main drivers of zooplankton community structure in the epipelagic layer. Therefore, our observations fall in line with the theory described above: in the epipelagic layers, less abundant and more diverse zooplankton thrive in warm, pico- and nanophytoplankton-dominated waters contrary to the polar waters where zooplankton is much more abundant but less diverse. Polar waters are characterised by a higher contribution of microphytoplankton to total phytoplankton biomass and higher concentrations of particles. Our results also indicate that the two polar communities are not completely alike, as the Arctic is dominated by calanoid copepods while euphausiids and small undetermined copepods dominate in the few stations sampled in the Southern Ocean. Such differentiation has been previously shown by several authors who found that Arctic zooplankton were dominated by *Calanus* spp. (Balazy et al., 2018; Hirche and Mumm, 1992), whereas it was shown that

Antarctic zooplankton were dominated by euphausiids, small calanoids, cyclopoids (i.e. *Oithona* spp., *Oncaea* spp.) and salps (Park and Wormuth, 1993; Quetin et al., 1996; Ross et al., 2008).

Important environmental factors for the mesozooplankton community structure in the mesopelgic layer

The RDA displayed similar general patterns in both the upper and lower mesopelagic layers with the stations in the Indian Ocean (with low zooplankton concentration in low oxygen) and Arctic Ocean (with high zooplankton concentration in oxygenated conditions) being in all layers well separated from the other stations in the remaining ocean. The highest mesopelagic zooplankton concentrations were found at stations associated with high microphytoplankton concentrations in the epipelagic and high particle flux, suggesting a strong impact of surface production regime on the mesozooplankton in the mesopelagic (Hernández-León et al., 2020). The inter-basin differences in zooplankton concentration and community composition was slightly lower in the lower mesopelagic compared to the upper mesopelagic, probably due to the more homogeneous habitat (Fernández de Puelles et al., 2019).

In general, stations associated with anoxic or hypoxic conditions at midwater depth displayed lower zooplankton concentrations in the mesopelagic and different community composition from oxygenated layers. The stations that sampled the tropical OMZ showed higher proportions of gelatinous carnivorous zooplankton (Cnidaria), gelatinous filter feeders (Tunicata), Mollusca and small omnivorous grazers (Cladocera). Anoxic or strongly hypoxic conditions in the mesopelagic may have selected for those taxa adapted to low oxygen (Vaquer-Sunyer and Duarte, 2008). In mesopelagic oxygenated waters, the stations of the Tropical Pacific Ocean displayed a higher diversity stemming from the higher and relatively even abundances of large protists (i.e. Rhizaria and Foraminifera), chaetognaths, crustaceans (Ostracods, Euphausiacea, Eumalacostraca, Amphipoda), and various copepod families (Corycaeidae, Oithonidae, Oncaeidae, small Calanoida). These zooplankton communities were associated with oligotrophic conditions at surface (Fig. 4), lower zooplankton abundances, lower concentrations of suspended matter, weaker particle fluxes and weaker attenuation rates (Fig. 3B) and with stronger attenuation rates of organisms' abundances (Fig. 3A). Therefore, we evidence oligotrophic regimes where the zooplankton community constitutes a network of diverse taxa that is not as efficient at using the low amount of material fluxing. Our results are consistent with previous studies suggesting that those oligotrophic regimes can be relatively efficient at exporting the slow-sinking fraction of the little carbon that is produced in the surface

layers due to a low impact of zooplankton grazing on the sinking particles (Guidi et al., 2009; Henson et al., 2015). This could help explain why we found the lowest particle flux attenuation rates in the tropics.

Global vertical patterns of zooplankton and particle flux

The concentration and biomass of various zooplankton groups decreased with depth (Fig. S1), confirming the general trend of decreasing zooplankton abundance and biomass from the surface to 1000 m depth resolved (Fig. 2; Bode et al., 2018; Brugnano et al., 2012; Hernández-León et al., 2020; Koppelmann et al., 2005; Kosobokova and Hopcroft, 2010; Yamaguchi et al., 2004). Among these earlier studies, two models for the attenuation of zooplankton have been proposed: an exponential or a power model. Here, we used the power model (equation 1) because it was widely used to model vertical flux attenuation rates (Martin et al., 1987). Based on this power model, we observed rates of decrease in zooplankton abundance or biomass (Fig. 3) that were in the same range as those reported in the western Pacific Ocean (-1.52 to -1.41 for abundance and -1.32 to -1.10 for biomass, (Yamaguchi et al., 2002). Zooplankton abundance decreased more rapidly with depth than biomass as the average size of organisms increased with depth, confirming that the contribution of larger species increases with depth (Homma and Yamaguchi, 2010; Yamaguchi et al., 2002). Considering a larger latitudinal band than earlier studies who found weak regional or global patterns (Hernández-León et al., 2020; Puelles et al., 2019), we showed that the rates of zooplankton attenuation vary with latitude and to a lesser extent with oxygen concentrations (Fig. 3) and also in the opposite direction of the flux attenuation.

Stronger surface particle fluxes and vertical attenuation rates were found at higher latitudes where primary production is mainly ensured by the microphytoplankton and weaker flux and attenuation was found in the low latitude dominated by picophytoplankton (Fig.4). Such latitudinal pattern in particle attenuation rates results from the gradient in the production regime and has been observed quasi-systematically with imaging systems on global scales (Guidi et al., 2015), but also based on sediment traps (Berelson, 2001) or combining sediment traps with satellite-based estimates of primary production (Henson et al., 2012). However, several short-term experiments at selected sites from temperate to tropical latitudes of the Pacific and Atlantic, showed an opposite pattern with stronger flux and attenuation in cold and productive regions compared to inter-tropical oligotrophic (Buesseler et al., 2007; Marsay et al., 2015). The inconsistency of the observations is difficult to explain although it was noted that depth varying remineralisation due to varying temperature may reconcile the contrasted

519 results (Marsay et al., 2015). It is possible that some of the differences arise from the use of
520 different methodologies (instruments, time scale, global representation of the dataset) to address
521 the complexity of the processes to be measured simultaneously.
522 Such opposite pattern between A_Zoo and B_zoo in one hand and A_Flux in the other
523 hand supports the view that the abundant zooplankton community plays a crucial role in flux
524 attenuation in productive layers, by feeding and fragmenting the sinking material as suggested
525 in previous studies (Dilling and Alldredge, 2000; Lampitt et al., 1990; Sarah L. C. Giering et
526 al., 2014; Stemmann et al., 2004). However, on average and more importantly at high latitudes,
527 zooplankton attenuation rates were stronger than the vertical flux attenuation rates (Fig. 3)
528 indicating that zooplankton vertical zonation may be affected by other processes than the
529 resources provided by the flux of organic matter from the epipelagic layer. In the inter-tropical
530 OMZ regions, zooplankton vertical attenuation rates were maximum when the vertical
531 attenuation of the particle's flux was minimum. Previous studies have reported lower flux
532 attenuation rates in the OMZ of the Arabian Sea (Haake et al., 1992; Roullier et al., 2014), and
533 Eastern Tropical North Pacific (Cavan et al., 2017; Van Mooy et al., 2002). Lower zooplankton
534 activity together with reduced bacterial activity (Cram et al., 2021) would allow sinking
535 particles to transit through the OMZ core without being severely degraded (Wishner et al., 2008,
536 1995) .
537

538 **Sensitivity of plankton and vertical flux to contrasted oxygen conditions**

539 By comparing zooplankton communities from inter-tropical stations with those from
540 oxygenated mesopelagic layers to stations from OMZs, our analysis brought additional
541 evidence that change in zooplankton community composition may affect the efficiency of the
542 BCP. The zooplankton community sampled in the Indian Ocean OMZ displayed a particular
543 composition compared to the other samples, which is in line with the increasing number of
544 studies that document the profound impact of oxygen depletion on pelagic organisms (Ekau et
545 al., 2010; Hauss et al., 2016; Wishner et al., 2018). Our results underlined how the OMZ can
546 strongly reduce the abundance of several zooplankton groups (i.e. Calanoida, Euphausiacea,
547 Amphipoda, Ostracoda) that are outcompeted by more hypoxia-tolerant ones. We found that
548 tunicates (mostly Appendicularia), large protists (Collodaria and Foraminifera), polychaetes,
549 Oncaeidae, Oithinidae and to a lesser extent Cnidaria (jellyfishes) may tolerate OMZ
550 conditions, since their abundance at OMZ and at non-OMZ stations did not present significant
551 differences. All of these zooplankton groups have been reported as being able to thrive or

endure at low oxygen concentrations in various OMZs (Ekau et al., 2010; Hauss et al., 2016; Keister and Tuttle, 2013; Kiko and Hauss, 2019; Parris et al., 2014; Tutasi and Escribano, 2020; Werner and Buchholz, 2013; Wishner et al., 2020). Those "hypoxiphilic" or hypoxia-tolerant taxa display special adaptations that enable them to remain at extremely low oxygen concentrations where other zooplankton groups cannot, because they fail to meet their metabolic oxygen demand (Childress and Seibel, 1998; Seibel, 2011). Jellyfish and large protists benefit from their passive feeding tactics which are less oxygen-demanding than active cruising and filter feeding (Kiørboe, 2011). Indeed, hypoxia-tolerant taxa can also display behavioral adaptations that cut down the metabolic costs associated with active feeding or the active search for mates in the water column. Copepod species belonging to the Oncaeidae and Oithonidae families are known for performing ambush feeding tactics or to attach themselves on large detritus (Brun et al., 2017), which allows them to capture small preys or to feed on falling detritus at very low metabolic costs. Therefore, these less motile copepods frequently outcompete most of their calanoid congeners in OMZs and often co-occur with Appendicularia, as those discard particle-rich aggregates on which the copepods feed (Alldredge, 1972; Brun et al., 2017; Kiørboe, 2011). Other possible adaptations consist in the use of lipid storages and metabolic suppression(Wishner et al., 2020). Some organisms conduct a diapause in the OMZ for an extended period, allowing them to avoid foraging predators and to complete their life cycle (Arashkevich et al., 1996). Diapause reduces energetic costs and thus allows the organisms to survive in resource-depleted conditions. Metabolic suppression goes hand in hand with the diapause, but can also occur on shorter time scales, e.g. when organisms stay at OMZ depth during diel vertical migrations. Diapause and metabolic suppression are associated with reduced respiratory and locomotor activity. Feeding on and disruption of particles could therefore be reduced at OMZ depth not only due to the exclusion of many hypoxia intolerant zooplankton organisms, but also due to the reduced activity of those zooplankton organisms that can cope with OMZ conditions. The zooplankton groups we found to characterize the community inhabiting the hypoxic and anoxic layers are those that commonly outcompete others in OMZs worldwide. They could benefit from the likely future expansion of OMZ (Oschlies et al., 2018) and thus become increasingly abundant with future climate change. This would probably result in enhanced vertical particle flux in those regions. However, this requires further research as some of these organisms could already be living near their physiological hypoxia tolerance limits (Wishner et al., 2018).

Conclusions

Our study combined consistent and large-scale observations of zooplankton abundance, biomass and community composition with estimates of vertical particle fluxes obtained through imaging system pipelines. We showed that consistent observations can be obtained at a global level using in situ camera systems and precise net sampling in various ecosystems representative of different ocean conditions. In future surveys, consistently combining these techniques with acoustic and other bio-optical sensors will allow the measurement of the vertical and horizontal distribution of organisms with greater precision. We showed that the key environmental variables driving epipelagic mesozooplankton community structure at the global scale are temperature, phytoplankton biomass and phytoplankton key groups. In the mesopelagic layer, surface phytoplankton size classes, particle concentration, temperature and oxygen availability were identified as the main drivers of mesozooplankton community structure. Our work furthermore suggests that low attenuation of zooplankton abundance and biomass go in hand with high particle flux attenuation and vice versa.Such information is crucial for the parameterization of the next generation of marine ecosystem models that describe complex zooplankton-related processes based on coarse but increasingly numerous functional types. Such models suggest that surface phytoplankton biomass and size classes, the flux of particles and the oxygen content in the mesopelagic layer will all be affected further by global climate change. The fact that zooplankton communities are sensitive to those factors suggests that future climatic changes may profoundly alter zooplankton communities worldwide, at the surface but also in the deeper mesopelagic layer.

ACKNOWLEDGMENTS

Tara Oceans (which includes both the Tara Oceans and Tara Oceans Polar Circle expeditions) would not exist without the leadership of the Tara Ocean Foundation and the continuous support of 23 institutes (https://oceans.taraexpeditions.org/). This study is part of the “Ocean Plankton, Climate and Development” project funded by the French Facility for Global Environment (FFEM). Y.D.S. and M.C.B. received financial support from FFEM to execute the project. R.K acknowledges support support via a “Make Our Planet Great Again” grant of the French National Research Agency within the “Programme d’Investissements d’Avenir”; reference “ANR-19-MPGA-0012”. F.B. received support from ETH Zürich and the European Union’s Horizon 2020 research and innovation programme under grant agreement n°SEP-210591007. We further thank the commitment of the following sponsors: CNRS (in

particular Groupement de Recherche GDR3280 and the Research Federation for the Study of Global Ocean Systems Ecology and Evolution FR2022/Tara Oceans-GOSEE), the European Molecular Biology Laboratory (EMBL), the French Ministry of Research, and the French Government ‘‘Investissements d’Avenir’’ programs OCEANOMICS (ANR-11-BTBR-0008), the EMBRC-France (ANR-10-INBS-02). Funding for the collection and processing of the Tara Oceans data set was provided by NASA Ocean Biology and Biogeochemistry Program under grants NNX11AQ14G, NNX09AU43G, NNX13AE58G, and NNX15AC08G (to the University of Maine); the Canada Excellence research chair on remote sensing of Canada’s new Arctic frontier; and the Canada Foundation for Innovation. We also thank Agnès b. and Etienne Bourgois, the Prince Albert II de Monaco Foundation, the Veolia Foundation, Region Bretagne, Lorient Agglomeration, Serge Ferrari, Worldcourier, and KAUST for support and commitment. The global sampling effort was enabled by countless scientists and crew who sampled aboard the Tara from 2009–2013, and we thank MERCATOR-CORIOLIS and ACRI-ST for providing daily satellite data during the expeditions. We are also grateful to the countries who graciously granted sampling permission.

References

Alldredge, A.L., 1972. Abandoned larvacean houses : a unique food source in pelagic environment. Science 177, 885.

Andersen, V., Francois, F., Sardou, J., Picheral, M., Scotto, M., Nival, P., 1998. Vertical distributions of macroplankton and micronekton in the Ligurian and Tyrrhenian Seas (northwestern Mediterranean). Oceanologica Acta 21, 655–676.

Arashkevich, E., Drits, A., Timonin, A., 1996. Diapause in the life cycle of Calanoides carinatus (Kroyer),(Copepoda, Calanoida). Hydrobiologia 320, 197–208.

Balazy, K., Trudnowska, E., Wichorowski, M., Błachowiak-Samołyk, K., 2018. Large versus small zooplankton in relation to temperature in the Arctic shelf region. Polar Research 37, 1427409.

Banse, K., 1964. On the vertical distribution of zooplankton in the sea. Progress in oceanography 2, 53–125.

Beaugrand, G., Conversi, A., Atkinson, A., Cloern, J., Chiba, S., Fonda-Umani, S., Kirby, R.R., Greene, C.H., Goberville, E., Otto, S.A., Reid, P.C., Stemmann, L., Edwards, M., 2019. Prediction of unprecedented biological shifts in the global ocean. Nature Climate Change 9, 237-+. https://doi.org/10.1038/s41558-019-0420-1

Berelson, W.M., 2002. Particle settling rates increase with depth in the ocean. Deep-Sea Research Part Ii-Topical Studies in Oceanography 49, 237–251.

Berelson, W.M., 2001. The Flux of Particulate Organic Carbon Into the Ocean Interior: A Comparison of Four U.S. JGOFS Regional Studies. Oceanography 14, 59–67.

Biard, T., Stemmann, L., Picheral, M., Mayot, N., Vandromme, P., Hauss, H., Gorsky, G., Guidi, L., Kiko, R., Not, F., 2016. In situ imaging reveals the biomass of giant protists in the global ocean. Nature 532, 504-+. https://doi.org/10.1038/nature17652

Bode, M., Hagen, W., Cornils, A., Kaiser, P., Auel, H., 2018. Copepod distribution and biodiversity patterns from the surface to the deep sea along a latitudinal transect in the eastern Atlantic Ocean (24°N to 21°S). Progress in Oceanography 161, 66–77. https://doi.org/10.1016/j.pocean.2018.01.010

Böttger-Schnack, R., 1996. Vertical structure of small metazoan plankton, especially noncalanoid copepods. I. Deep Arabian Sea. Journal of Plankton Research 18, 1073–1101. https://doi.org/10.1093/plankt/18.7.1073

Brugnano, C., Granata, A., Guglielmo, L., Zagami, G., 2012. Spring diel vertical distribution of copepod abundances and diversity in the open Central Tyrrhenian Sea (Western Mediterranean). Journal of Marine Systems 105, 207–220.

Brun, P., Payne, M.R., Kiørboe, T., 2017. A trait database for marine copepods. Earth System Science Data 9, 99–113.

Buesseler, K.O., Lamborg, C.H., Boyd, P.W., Lam, P.J., Trull, T.W., Bidigare, R.R., Bishop, J.K.B., Casciotti, K.L., Dehairs, F., Elskens, M., Honda, M., Karl, D.M., Siegel, D.A., Silver, M.W., Steinberg, D.K., Valdes, J., Van Mooy, B., Wilson, S., 2007. Revisiting Carbon Flux Through the Ocean's Twilight Zone. Science 316, 567–570. https://doi.org/10.1126/science.1137959

Cavan, E.L., Henson, S.A., Belcher, A., Sanders, R., 2017. Role of zooplankton in determining the efficiency of the biological carbon pump. Biogeosciences 14, 177–186.

Childress, J.J., Seibel, B.A., 1998. Life at stable low oxygen levels: adaptations of animals to oceanic oxygen minimum layers. The Journal of experimental biology 201, 1223–1232.

Chust, G., Allen, J.I., Bopp, L., Schrum, C., Holt, J., Tsiaras, K., Zavatarelli, M., Chifflet, M., Cannaby, H., Dadou, I., 2014. Biomass changes and trophic amplification of

plankton in a warmer ocean. Global Change Biology 20, 2124–2139.
Coma, R., Ribes, M., Serrano, E., Jiménez, E., Salat, J., Pascual, J., 2009. Global warming-enhanced stratification and mass mortality events in the Mediterranean. Proceedings of the National Academy of Sciences 106, 6176–6181.
Cram, J., Fuchsman, C., Duffy, M., Pretty, J., Lekanoff, R., Neibauer, J., Leung, S., Huebert, K.B., Weber, T., Bianchi, D., 2021. Slow particle remineralization, rather than suppressed disaggregation, drives efficient flux transfer through the Eastern Tropical North Pacific Oxygen Deficient Zone. Earth and Space Science Open Archive ESSOAr.
Dilling, L., Alldredge, A.L., 2000. Fragmentation of marine snow by swimming macrozooplankton: A new process impacting carbon cycling in the sea. Deep-Sea Research Part I-Oceanographic Research Papers 47, 1227–1245.
Ekau, W., Auel, H., Portner, H.O., Gilbert, D., 2010. Impacts of hypoxia on the structure and processes in pelagic communities (zooplankton, macro-invertebrates and fish). Biogeosciences 7, 1669–1699. https://doi.org/10.5194/bg-7-1669-2010
Everett, J.D., Baird, M.E., Buchanan, P., Bulman, C., Davies, C., Downie, R., Griffiths, C., Heneghan, R., Kloser, R.J., Laiolo, L., 2017. Modeling what we sample and sampling what we model: challenges for zooplankton model assessment. Frontiers in Marine Science 4, 77.
Fernández de Puelles, M., Gazá, M., Cabanellas-Reboredo, M., Santandreu, M., Irigoien, X., González-Gordillo, J.I., Duarte, C.M., Hernández-León, S., 2019. Zooplankton abundance and diversity in the tropical and subtropical ocean. Diversity 11, 203.
Forest, A., Babin, M., Stemmann, L., Picheral, M., Sampei, M., Fortier, L., Gratton, Y., Belanger, S., Devred, E., Sahlin, J., Doxaran, D., Joux, F., Ortega-Retuerta, E., Martin, J., Jeffrey, W.H., Gasser, B., Miquel, J.C., 2013. Ecosystem function and particle flux dynamics across the Mackenzie Shelf (Beaufort Sea, Arctic Ocean): an integrative analysis of spatial variability and biophysical forcings. Biogeosciences 10, 2833–2866. https://doi.org/10.5194/bg-10-2833-2013
Gaard, E., Gislason, A., Falkenhaug, T., Søiland, H., Musaeva, E., Vereshchaka, A., Vinogradov, G., 2008. Horizontal and vertical copepod distribution and abundance on the Mid-Atlantic Ridge in June 2004. Deep Sea Research Part II: topical studies in oceanography 55, 59–71.
Gallienne, C.P., Robins, D.B., Woodd-Walker, R.S., 2001. Abundance, distribution and size structure of zooplankton along a 20 degrees west meridional transect of the northeast Atlantic Ocean in July. Deep-Sea Research Part Ii-Topical Studies in Oceanography 48, 925–949.
Gehlen, M., Bopp, L., Ernprin, N., Aumont, O., Heinze, C., Raguencau, O., 2006. Reconciling surface ocean productivity, export fluxes and sediment composition in a global biogeochemical ocean model. Biogeosciences 3, 521–537.
Guidi, L., Chaffron, S., Bittner, L., Eveillard, D., Larhlimi, A., Roux, S., Darzi, Y., Audic, S., Berline, L., Brum, J.R., Coelho, L.P., Espinoza, J.C.I., Malviya, S., Sunagawa, S., Dimier, C., Kandels-Lewis, S., Picheral, M., Poulain, J., Searson, S., Stemmann, L., Not, F., Hingamp, P., Speich, S., Follows, M., Karp-Boss, L., Boss, E., Ogata, H., Pesant, S., Weissenbach, J., Wincker, P., Acinas, S.G., Bork, P., de Vargas, C., Iudicone, D., Sullivan, M.B., Raes, J., Karsenti, E., Bowler, C., Gorsky, G., Tara Oceans Consortium Coordinator, 2016. Plankton networks driving carbon export in the oligotrophic ocean. Nature 532, 465-+.
Guidi, L., Jackson, G.A., Stemmann, L., Miquel, J.C., Picheral, M., Gorsky, G., 2008. Relationship between particle size distribution and flux in the mesopelagic zone. Deep-Sea Research Part I-Oceanographic Research Papers 55, 1364–1374.

Guidi, L., Legendre, L., Reygondeau, G., Uitz, J., Stemmann, L., Henson, S.A., 2015. A new look at ocean carbon remineralization for estimating deepwater sequestration. Global Biogeochem. Cycles 29, 1044–1059. https://doi.org/10.1002/2014gb005063

Guidi, L., Stemmann, L., Jackson, G.A., Ibanez, F., Claustre, H., Legendre, L., Picheral, M., Gorsky, G., 2009. Effects of phytoplankton community on production, size and export of large aggregates: A world-ocean analysis. Limnology and Oceanography 54, 1951–1963. https://doi.org/10.4319/lo.2009.54.6.1951

Haake, B., Ittekkot, V., Ramaswamy, V., Nair, R., Honjo, S., 1992. Fluxes of amino acids and hexosamines to the deep Arabian Sea. Marine Chemistry 40, 291–314.

Hauss, H., Christiansen, S., Schütte, F., Kiko, R., Edvam Lima, M., Rodrigues, E., Karstensen, J., Löscher, C.R., Körtzinger, A., Fiedler, B., 2016. Dead zone or oasis in the open ocean? Zooplankton distribution and migration in low-oxygen modewater eddies. Biogeosciences 13, 1977–1989.

Henson, S.A., Sanders, R., Madsen, E., 2012. Global patterns in efficiency of particulate organic carbon export and transfer to the deep ocean. Global Biogeochemical Cycles 26.

Henson, S.A., Yool, A., Sanders, R., 2015. Variability in efficiency of particulate organic carbon export: A model study. Global Biogeochemical Cycles 29, 33–45.

Hernández-León, S., Koppelmann, R., Fraile-Nuez, E., Bode, A., Mompeán, C., Irigoien, X., Olivar, M.P., Echevarría, F., de Puelles, M.F., González-Gordillo, J.I., 2020. Large deep-sea zooplankton biomass mirrors primary production in the global ocean. Nature communications 11, 1–8.

Hidalgo, P., Escribano, R., Fuentes, M., Jorquera, E., Vergara, O., 2012. How coastal upwelling influences spatial patterns of size-structured diversity of copepods off central-southern Chile (summer 2009). Progress in Oceanography 92, 134–145.

Hirche, H.-J., Mumm, N., 1992. Distribution of dominant copepods in the Nansen Basin, Arctic Ocean, in summer. Deep Sea Research Part A. Oceanographic Research Papers 39, S485–S505.

Homma, T., Yamaguchi, A., 2010. Vertical changes in abundance, biomass and community structure of copepods down to 3000 m in the southern Bering Sea. Deep Sea Research Part I: Oceanographic Research Papers 57, 965–977.

Ibarbalz, F.M., Henry, N., Brandao, M.C., Martini, V., Busseni, G., Byrne, H., Coelho, L.P., Endo, H., Gasol, J.M., Gregory, A.C., Mahe, F., Rigonato, J., Royo-Llonch, M., Salazar, G., Sanz-Saez, I., Scalco, E., Soviadan, D., Zayed, A.A., Zingone, A., Labadie, K., Ferland, J., Marec, C., Kandels, S., Picheral, M., Dimier, C., Poulain, J., Pisarev, S., Carmichael, M., Pesant, S., Acinas, S.G., Babin, M., Bork, P., Boss, E., Bowler, C., Cochrane, G., de Vargas, C., Follows, M., Gorsky, G., Grimsley, N., Guidi, L., Hingamp, P., Iudicone, D., Jaillon, O., Kandels, S., Karp-Boss, L., Karsenti, E., Not, F., Ogata, H., Pesant, S., Poulton, N., Raes, J., Sardet, C., Speich, S., Stemmann, L., Sullivan, M.B., Sunagawa, S., Wincker, P., Bopp, L., Lombard, F., Zinger, L., Tara Oceans, C., 2019. Global Trends in Marine Plankton Diversity across Kingdoms of Life. Cell 179, 1084-+. https://doi.org/10.1016/j.cell.2019.10.008

Irigoien, X., Klevjer, T.A., Røstad, A., Martinez, U., Boyra, G., Acuña, J.L., Bode, A., Echevarria, F., Gonzalez-Gordillo, J.I., Hernandez-Leon, S., 2014. Large mesopelagic fishes biomass and trophic efficiency in the open ocean. Nature communications 5, 1–10.

Iversen, M.H., Lampitt, R.S., 2020. Size does not matter after all: no evidence for a size-sinking relationship for marine snow. Progress in Oceanography 189, 102445.

Karsenti, E., Acinas, S.G., Bork, P., Bowler, C., De Vargas, C., Raes, J., Sullivan, M., Arendt, D., Benzoni, F., Claverie, J.M., Follows, M., Gorsky, G., Hingamp, P.,

Iudicone, D., Jaillon, O., Kandels-Lewis, S., Krzic, U., Not, F., Ogata, H., Pesant, S., Reynaud, E.G., Sardet, C., Sieracki, M.E., Speich, S., Velayoudon, D., Weissenbach, J., Wincker, P., Tara Oceans, C., 2011. A Holistic Approach to Marine Eco-Systems Biology. Plos Biology 9. https://doi.org/e1001177 10.1371/journal.pbio.1001177

Keister, J.E., Tuttle, L.B., 2013. Effects of bottom-layer hypoxia on spatial distributions and community structure of mesozooplankton in a sub-estuary of Puget Sound, Washington, USA. Limnology and Oceanography 58, 667–680.

Kiko, R., Biastoch, A., Brandt, P., Cravatte, S., Hauss, H., Hummels, R., Kriest, I., Marin, F., McDonnell, A.M.P., Oschlies, A., Picheral, M., Schwarzkopf, F.U., Thurnherr, A.M., Stemmann, L., 2017. Biological and physical influences on marine snowfall at the equator. Nature Geoscience 10, 852-+. https://doi.org/10.1038/ngeo3042

Kiko, R., Brandt, P., Christiansen, S., Faustmann, J., Kriest, I., Rodrigues, E., Schütte, F., Hauss, H., 2020. Zooplankton-mediated fluxes in the eastern tropical North Atlantic. Frontiers in Marine Science 1.

Kiko, R., Hauss, H., 2019. On the estimation of zooplankton-mediated active fluxes in oxygen minimum zone regions. Frontiers in Marine Science 6, 741.

Kiørboe, T., 2013. Zooplankton body composition. Limnology and Oceanography 58, 1843–1850.

Kiørboe, T., 2011. What makes pelagic copepods so successful? Journal of Plankton Research 33, 677–685.

Kiørboe, T., Visser, A., Andersen, K.H., Handling editor: Howard Browman, 2018. A trait-based approach to ocean ecology. ICES Journal of Marine Science. https://doi.org/10.1093/icesjms/fsy090

Koppelmann, R., Weikert, H., Halsband-Lenk, C., Jennerjahn, T., 2004. Mesozooplankton community respiration and its relation to particle flux in the oligotrophic eastern Mediterranean. Global Biogeochemical Cycles 18.

Koppelmann, R., Zimmermann-Timm, H., Weikert, H., 2005. Bacterial and zooplankton distribution in deep waters of the Arabian Sea. Deep-Sea Research Part I-Oceanographic Research Papers 52, 2184–2192. https://doi.org/10.1016/j.dsr.2005.06.012

Kosobokova, K.N., Hopcroft, R.R., 2010. Diversity and vertical distribution of mesozooplankton in the Arctic's Canada Basin. Deep Sea Research Part II: Topical Studies in Oceanography 57, 96–110.

Kwiatkowski, L., Aumont, O., Bopp, L., 2019. Consistent trophic amplification of marine biomass declines under climate change. Global change biology 25, 218–229.

Lampitt, R.S., Noji, T., Von Bodungen, B., 1990. What happens to zooplankton fecal pellets ? Implication for material flux. Marine Biology 104, 15–23.

Laws, R.M., 1985. The ecology of the Southern Ocean. Amer. Scient. 73, 26–40.

Legendre, P., Legendre, L., 1998. Numerical ecology, 2nd english. ed, Developments in environmental modelling 20. Elsevier, Amsterdam.

Lehette, P., Hernandez-Leon, S., 2009. Zooplankton biomass estimation from digitized images: a comparison between subtropical and Antarctic organisms. Limnology and Oceanography-Methods 7, 304–308.

Madhupratap, M., Nair, KNV, Venugopal, P., Gauns, M., Haridas, P., Gopalakrishnan, T., Nair, KKC, 2004. Arabian Sea oceanography and fisheries.

Marsay, C.M., Sanders, R.J., Henson, S.A., Pabortsava, K., Achterberg, E.P., Lampitt, R.S., 2015. Attenuation of sinking particulate organic carbon flux through the mesopelagic ocean. Proceedings of the National Academy of Sciences 112, 1089–1094.

Martin, J.H., Knauer, G.A., Karl, D.M., Broenkow, W.W., 1987. VERTEX: Carbon

cycling in the Northeast Pacific. Deep-Sea Research 34, 267–285.
Morrison, J.M., Codispoti, L., Smith, S.L., Wishner, K., Flagg, C., Gardner, W.D., Gaurin, S., Naqvi, S., Manghnani, V., Prosperie, L., 1999. The oxygen minimum zone in the Arabian Sea during 1995. Deep Sea Research Part II: Topical Studies in Oceanography 46, 1903–1931.
MOTODA, S., 1959. Devices of simple plankton apparatus. Memoirs of the faculty of fisheries Hokkaido University 7, 73–94.
Ohman, M.D., Romagnan, J.B., 2016. Nonlinear effects of body size and optical attenuation on Diel Vertical Migration by zooplankton. Limnology and Oceanography 61, 765–770. https://doi.org/10.1002/lno.10251
Oschlies, A., Brandt, P., Stramma, L., Schmidtko, S., 2018. Drivers and mechanisms of ocean deoxygenation. Nature Geoscience 11, 467–473.
Paffenhofer, G.A., Mazzocchi, M.G., 2003. Vertical distribution of subtropical epiplanktonic copepods. Journal of Plankton Research 25, 1139–1156.
Palomares-García, R.J., Gómez-Gutiérrez, J., Robinson, C.J., 2013. Winter and summer vertical distribution of epipelagic copepods in the Gulf of California. Journal of Plankton Research 35, 1009–1026.
Park, C., Wormuth, J., 1993. Distribution of Antarctic zooplankton around Elephant Island during the austral summers of 1988, 1989, and 1990. Polar Biology 13, 215–225.
Parris, D.J., Ganesh, S., Edgcomb, V.P., DeLong, E.F., Stewart, F.J., 2014. Microbial eukaryote diversity in the marine oxygen minimum zone off northern Chile. Frontiers in microbiology 5, 543.
Pesant, S., Not, F., Picheral, M., Kandels-Lewis, S., Le Bescot, N., Gorsky, G., Iudicone, D., Karsenti, E., Speich, S., Trouble, R., Dimier, C., Searson, S., Tara Oceans Consortium, C., 2015. Open science resources for the discovery and analysis of Tara Oceans data. Scientific data 2, 150023–150023. https://doi.org/10.1038/sdata.2015.23
Quetin, L.B., Ross, R.M., Frazer, T.K., Haberman, K.L., 1996. Factors affecting distribution and abundance of zooplankton, with an emphasis on Antarctic krill, Euphausia superba. Antarctic Research Series 70, 357–371.
Remsen, A., Hopkins, T.L., Samson, S., 2004. What you see is not what you catch: a comparison of concurrently collected net, Optical Plankton Counter, and Shadowed Image Particle Profiling Evaluation Recorder data from the northeast Gulf of Mexico. Deep-Sea Research Part I-Oceanographic Research Papers 51, 129–151.
Richardson, A.J., 2008. In hot water: zooplankton and climate change. ICES Journal of Marine Science 65, 279–295. https://doi.org/10.1093/icesjms/fsn028
Robinson, C., Steinberg, D.K., Anderson, T.R., Aristegui, J., Carlson, C.A., Frost, J.R., Ghiglione, J.F., Hernandez-Leon, S., Jackson, G.A., Koppelmann, R., Queguiner, B., Ragueneau, O., Rassoulzadegan, F., Robison, B.H., Tamburini, C., Tanaka, T., Wishner, K.F., Zhang, J., 2010. Mesopelagic zone ecology and biogeochemistry - a synthesis. Deep-Sea Research Part Ii-Topical Studies in Oceanography 57, 1504–1518. https://doi.org/10.1016/j.dsr2.2010.02.018
Roe, H., 1988. Midwater biomass profiles over the Madeira Abyssal Plain and the contribution of copepods, in: Biology of Copepods. Springer, pp. 169–181.
Rombouts, I., Beaugrand, G., Ibanez, F., Gasparini, S., Chiba, S., Legendre, L., 2010. A multivariate approach to large-scale variation in marine planktonic copepod diversity and its environmental correlates. Limnology and Oceanography 55, 2219–2229. https://doi.org/10.4319/lo.2010.55.5.2219
Ross, R.M., Quetin, L.B., Martinson, D.G., Iannuzzi, R.A., Stammerjohn, S.E., Smith, R.C., 2008. Palmer LTER: Patterns of distribution of five dominant zooplankton

883 species in the epipelagic zone west of the Antarctic Peninsula, 1993–2004. Deep Sea
884 Research Part II: Topical Studies in Oceanography 55, 2086–2105.
885 Roullier, F., Berline, L., Guidi, L., De Madron, X.D., Picheral, M., Sciandra, A., Pesant,
886 S., Stemmann, L., 2014. Particle size distribution and estimated carbon flux across the
887 Arabian Sea oxygen minimum zone. Biogeosciences 11, 4541–4557.
888 https://doi.org/10.5194/bg-11-4541-2014
889 Rutherford, S., D'Hondt, S., Prell, W., 1999. Environmental controls on the geographic
890 distribution of zooplankton diversity. Nature 400, 749–753.
891 https://doi.org/10.1038/23449
892 Saporiti, F., Bearhop, S., Vales, D.G., Silva, L., Zenteno, L., Tavares, M., Crespo, E.A.,
893 Cardona, L., 2015. Latitudinal changes in the structure of marine food webs in the
894 Southwestern Atlantic Ocean. Marine Ecology Progress Series 538, 23–34.
895 Sarah L. C. Giering, Richard Sanders, Richard S. Lampitt, Thomas R. Anderson,
896 Christian Tamburini, Mehdi Boutrif, Mikhail V. Zubkov, Chris M. Marsay, Stephanie
897 A. Henson, Kevin Saw, Kathryn Cook, Daniel J. Mayor, 2014. Reconciliation of the
898 carbon budget in the ocean's twilight zone. Nature 507, 17.
899 https://doi.org/10.1038/nature13123
900 Schmidtko, S., Stramma, L., Visbeck, M., 2017. Decline in global oceanic oxygen content
901 during the past five decades. Nature 542, 335–339.
902 Seibel, B.A., 2011. Critical oxygen levels and metabolic suppression in oceanic oxygen
903 minimum zones. Journal of Experimental Biology 214, 326–336.
904 Smith, S., Roman, M., Prusova, I., Wishner, K., Gowing, M., Codispoti, L.A., Barber, R.,
905 Marra, J., Flagg, C., 1998. Seasonal response of zooplankton to monsoonal reversals
906 in the Arabian Sea. Deep-Sea Research Part II 45, 2369–2403.
907 St John, M.A., Borja, A., Chust, G., Heath, M., Grigorov, I., Mariani, P., Martin, A.P.,
908 Santos, R.S., 2016. A dark hole in our understanding of marine ecosystems and their
909 services: perspectives from the mesopelagic community. Frontiers in Marine Science
910 3, 31.
911 Steinberg, D.K., Landry, M.R., 2017. Zooplankton and the ocean carbon cycle. Annual
912 review of marine science 9, 413–444.
913 Stemmann, L., Jackson, G.A., Gorsky, G., 2004. A vertical model of particle size
914 distributions and fluxes in the midwater column that includes biological and physical
915 processes - Part II: application to a three year survey in the NW Mediterranean Sea.
916 Deep-Sea Research Part I-Oceanographic Research Papers 51, 885–908.
917 https://doi.org/10.1016/j.dsr.2004.03.002
918 Stempniewicz, L., Błachowiak-Samołyk, K., Węsławski, J.M., 2007. Impact of climate
919 change on zooplankton communities, seabird populations and arctic terrestrial
920 ecosystem—a scenario. Deep Sea Research Part II: Topical Studies in Oceanography
921 54, 2934–2945.
922 Stramma, L., Schmidtko, S., Levin, L.A., Johnson, G.C., 2010. Ocean oxygen minima
923 expansions and their biological impacts. Deep Sea Research Part I: Oceanographic
924 Research Papers 57, 587–595. https://doi.org/10.1016/j.dsr.2010.01.005
925 Stukel, M.R., Ohman, M.D., Kelly, T.B., Biard, T., 2019. The roles of suspension-feeding
926 and flux-feeding zooplankton as gatekeepers of particle flux into the mesopelagic
927 ocean in the Northeast Pacific. Frontiers in Marine Science 6, 397.
928 Tarling, G.A., Shreeve, R.S., Ward, P., Atkinson, A., Hirst, A.G., 2004. Life-cycle
929 phenotypic composition and mortality of Calanoides acutus (Copepoda : Calanoida) in
930 the Scotia Sea: a modelling approach. Marine Ecology-Progress Series 272, 165–181.
931 Terazaki, M., Wada, M., 1988. Occurrence of large numbers of carcasses of the large,
932 grazing copepod Calanus cristatus from the Japan Sea. Marine Biology 97, 177–183.

Trudnowska, E., Lacour, L., Ardyna, M., Rogge, A., Irisson, J.O., Waite, A.M., Babin, M., Stemmann, L., 2021. Marine snow morphology illuminates the evolution of phytoplankton blooms and determines their subsequent vertical export. Nature communications 12, 2816–2816. https://doi.org/10.1038/s41467-021-22994-4

Tutasi, P., Escribano, R., 2020. Zooplankton diel vertical migration and downward C flux into the oxygen minimum zone in the highly productive upwelling region off northern Chile. Biogeosciences 17, 455–473.

Uitz, J., Claustre, H., Morel, A., Hooker, S.B., 2006. Vertical distribution of phytoplankton communities in open ocean: An assessment based on surface chlorophyll. Journal of Geophysical Research. C. Oceans 111, [doi:10.1029/2005JC003207].

Van Mooy, B.A., Keil, R.G., Devol, A.H., 2002. Impact of suboxia on sinking particulate organic carbon: Enhanced carbon flux and preferential degradation of amino acids via denitrification. Geochimica et Cosmochimica Acta 66, 457–465.

Vaquer-Sunyer, R., Duarte, C.M., 2008. Thresholds of hypoxia for marine biodiversity. Proceedings of the National Academy of Sciences 105, 15452–15457.

Werner, T., Buchholz, F., 2013. Diel vertical migration behaviour in Euphausiids of the northern Benguela current: seasonal adaptations to food availability and strong gradients of temperature and oxygen. Journal of Plankton Research 35, 792–812.

Wheeler Jr, E., 1967. Copepod detritus in the deep sea. Limnology and Oceanography 12, 697–702.

Wishner, K.F., Ashjian, C.J., Gelfman, C., Gowing, M.M., Kann, L., Levin, L.A., Mullineaux, L.S., Saltzman, J., 1995. Pelagic and Benthic Ecology of the Lower Interface of the Eastern Tropical Pacific Oxygen Minimum Zone. Deep Sea Res. 42, 93–115.

Wishner, K.F., Gelfman, C., Gowing, M.M., Outram, D.M., Rapien, M., Williams, R.L., 2008. Vertical zonation and distributions of calanoid copepods through the lower oxycline of the Arabian Sea oxygen minimum zone. Prog. Oceanogr. 78, 163–191. https://doi.org/10.1016/j.pocean.2008.03.001

Wishner, K.F., Seibel, B., Outram, D., 2020. Ocean deoxygenation and copepods: coping with oxygen minimum zone variability. Biogeosciences 17, 2315–2339.

Wishner, K.F., Seibel, B.A., Roman, C., Deutsch, C., Outram, D., Shaw, C.T., Birk, M.A., Mislan, K., Adams, T., Moore, D., 2018. Ocean deoxygenation and zooplankton: very small oxygen differences matter. Science advances 4, eaau5180.

Yamaguchi, A., Watanabe, Y., Ishida, H., Harimoto, T., Furusawa, K., Suzuki, S., Ishizaka, J., Ikeda, T., Mac Takahashi, M., 2004. Latitudinal differences in the planktonic biomass and community structure down to the greater depths in the western North Pacific. Journal of Oceanography 60, 773–787.

Yamaguchi, A., Watanabe, Y., Ishida, H., Harimoto, T., Furusawa, K., Suzuki, S., Ishizaka, J., Ikeda, T., Takahashi, M., 2002. Community and trophic structures ofpelagic copepods down to greater depths in the western subarctic Paci fic (WEST-COSMIC). Deep Sea Research Part I 49, 1007–1025.

Yasuhara, M., Hunt, G., Dowsett, H.J., Robinson, M.M., Stoll, D.K., 2012. Latitudinal species diversity gradient of marine zooplankton for the last three million years. Ecology Letters 15, 1174–1179. https://doi.org/10.1111/j.1461-0248.2012.01828.x

983

984 Table 1: List of the 19 taxa kept for the RDA analysis.

Taxonomic groups	Sub groups
Protista	Protista includes unrecognized protista on the images
Annelida	Images of all Annelida
Chaetognatha	Images of all Chaetognatha
Tunicata	Images of all Gelatinous filter feeders
Cnidaria	Images of all gelatinous carnivores belonging to Cnidaria
Mollusca	Images of all Pteropoda
Cladocera	Images of all Small Cladocera
Eumalacostraca	Images of all Decapoda but those distinguish at detailed taxonomic level
Euphausiacea	Images of all Euphausiacea
Amphipoda	Images of all Amphipoda
Ostracoda	Images of all Ostracoda
Crustacean_larvae	Images of all crustacean larvae
Other_Copepoda	Images of all Copepoda but those distinguish at detailed taxonomic level
Calanoida	Images of all Calanoida but those distinguish at detailed taxonomic level
Oithonidae	Images of all Oithonidae
Corycaeidae	Images of all Corycaeidae
Oncaeidae	Images of all Oncaeidae
Metridinidae	Images of all Metridinidae
Calanidae	Images of all Calanidae

985

986 Table 2: Coefficient factors used for equation 1 and that were taken from observed allometric
987 relationships between body area and individual dry mass (Lehette et al., 2009). The conversion factors
988 to carbon are taken from Kiorboe 2013.

Zooplankton category	Biomass Exponent (*b*)	Biomass Multiplier (*a*)	DW to C
Copepods	1.59 ± 0.03	45.25	0.48
Chaetognaths	1.19 ± 0.13	23.45	0.367
Decapods	1.48 ± 0.05	49.58	0.419
Cnidaria	1.02 ± 0.38	43.17	0.132
Tunicata	1.24 ± 0.08	4.03	0.103
Pteropods	1.54 ± 0.03	43.38	0.289
Protists*		0.08 mgC mm-3	
Other (Annelids, Cladocera, Ostracoda)	1.54 ± 0.03	43.38	0.289

989 * for the protist we used a conversion factor between biovolume and biomass (Biard et al.,
990 2016)
991

Table 3: Summary of the main mesozooplankton groups global proportion of abundance and biomass:

Taxa Proportion(%)	Epipelagic		Upper Mesopelagic		Lower Mesopelagic	
	Abundance	**Biomass**	**Abundance**	**Biomass**	**Abundance**	**Biomass**
All copepoda	84.89	65	84.80	76.39	94.5	96.5
Chaetognatha	3.67	8.39	2.44	3.48	2.06	2.53
Crust decapoda	2.9	18.9	0.36	14.98	0.00	0.00
Cnidaria	0.7	0.96	0.19	0.24	0.00	0.00
Tunicata	0.5	0.02	0.08	0.001	0.1	0.00
Protista	1.5	0.5	0.97	0.19	0.9	0.09
Pteropoda	1.2	0.6	0.41	0.03	0.00	0.00
Other (annelids, cladocera, ostracoda)	4.2	3.09	10.05	3.23	2.38	0.87

Table 4: Summary of the vertical attenuation rate (b: median and IC: confidence Interval) of mesozooplankton abundance and biomass and particle vertical flux (b: median value and IC: confidence Interval).

	Zooplankton abundance $(Ind.m^{-3})$		**Zooplankton biomass** $(mgC.m^{-3})$		**Particle vertical flux**	
	b	IC (95%)	*b*	IC (95%)	*b*	IC (95%)
ANOXIA_TROPIC	-1.82	-2.13 - -1.13	-1.3	-2.9 - -0.75	-0.26	-0.77- -0.19
TROPIC	-1.39	-2.46 - -0.69	-1.04	-1.92 - -0.58	-0.42	-0.78- -0.21
TEMPERATE	-1.19	-1.56 - -0.64	-0.89	-1.26 - -0.57	-0.50	-0.84- -0.11
POLAR	-1.18	-1.71 - -0.96	-0.83	-1.41 - -0.74	-0.78	-4.51- -0.36

Table 5: Probability of H0, no difference between the groups (pairwise Kruskal-Wallis test) for total zooplankton and biomass depth attenuation rates and particle flux attenuation rate. * Significant differences.

Two by two comparisons		**Abundance**	**Biomass**	**Flux**
Tropic-Anoxia	Tropic	0.057	0.641	0.77
Tropic-Anoxia	Temperate	0.0018*	0.189	0.82
Tropic-Anoxia	Polar	0.01*	0.238	0.09
Tropic	Temperate	0.34	0.639	0.99
Tropic	Polar	0.51	0.685	0.28
Temperate	Polar	0.99	1	0.52

Supplementary material

Availability of the dataset

Data sets for the environment are available at Pangea:

(https://doi.org/10.1594/PANGAEA.840721)

Tables for the RDA are available

For zooplankton: Metadata_Zooplankton_Article_RDA.xls

Zooplankton Pangea for the tables/ecotaxa for the vignettes

https://ecotaxa.obs-vlfr.fr/prj/714?taxo=56693&taxochild=N&ipp=100&zoom=100&sortby=&magenabled=0&popupenabled=0&statusfilter=&samples=&instrum=&sortorder=asc&dispfield=&projid=714&pageoffset=0

Quality of the dataset

The analysis reported here is the first to apply consistent imaging techniques in order to investigate particle flux, zooplankton community composition and biomass across the global ocean. To do so, our study relies on the combined use of the Underwater Video Profiler v5 (UVP5), a Multinet and the Zooscan imaging system. These results are the first combined global zooplankton and flux estimates and as such provide a baseline for future studies. Their quality needs to be discussed with regards to 1) flux assessment, 2) mesh selectivity, mass conversion and possible impact of dead zooplankton in the images, the capacity of the sampling design to capture or not 3) day night variability and 4) mesopelagic peaks of zooplankton.

Vertical particle mass fluxes (mg Dry Weight $m^{-2}d^{-1}$) were calculated from the particle size spectra (150 µm -1.5 mm) detected by the UVP5 following Guidi et al., (2008). Briefly, the procedure optimized two parameters in the flux equation by comparing UVP5 derived flux and a global sediment trap flux data set (Guidi et al., 2008). Depending on the ocean basin, regional algorithms with different sets of the two parameters have been proposed (Forest et al., 2013; Kiko et al., 2017) but the shape of the allometric relationships between particle size and flux is kept as a growing monotonic power relationship. Many studies have shown that this assumption is verified when comparing extremes size of particles but they all have also shown

a high variability (Guidi et al., 2008; Iversen and Lampitt, 2020) which cannot be depicted without more information on the type of particles. In addition, we used the same parametrization for each depth layer although a few observational and modelling studies (Berelson, 2002; Gehlen et al., 2006) have proposed that the sinking speed may vary with depth. Finally, the fluxes are calculated considering all particles detected in situ by the UVP5. Because particles are so abundant in the size range presently considered for flux estimation (150µm to 1.5mm), the impact of zooplankton in the present flux estimates is low (Guidi et al., 2015; Kiko et al., 2020). We did not perform further sensitivity analyses as the aim of this study was not to quantify absolute carbon flux but to assess correlations with zooplankton and other environmental variables. In the future, better recognition of particles on images will possibly allow to calculate different particle speed for different ypes of aggregates as was proposed recently (Trudnowska et al., 2021).

Zooplankton abundance estimates are sensitive to the mesh of the plankton net tow used (Gallienne et al., 2001). A mesh size of 300µm was selected for the Multinet as a good compromise to capture both mesozooplankton and macro-zooplankton. However, the small copepod families (Oithona, Oncaeidae, Clausocalanidae, Paracalanidae) that dominate community composition in tropical/subtropical open oceans are not collected in an optimal fashion with the present mesh size, contrary to the larger Calanidae notably in the temperate and polar regions. Therefore, our abundance estimates likely underestimate the contribution of the smallest mesozooplankton groups. Nonetheless, even a net equipped with a 150 µm mesh can still underestimate the abundance of cyclopoids and early copepod stages (Paffenhofer and Mazzocchi, 2003).

Nets can also destroy fragile organisms during the sampling process (Remsen et al., 2004). For example, the very low abundance and biomass of Rhizarians reported here contrasting with recent findings based on *in situ* cameras (Biard et al., 2016). This is likely due to such sampling biases. As for the estimation of particle fluxes from particle size spectra, we assessed the carbon biomass of each individual organism's size using published allometric relationships (Lehette and Hernández-León, 2009) in which large and rare organisms contributes importantly to the total biomass bringing strong variability in the results. To account for the excessive variability in biomass estimates, we analysed our results using both abundance and biomass.

Dead zooplankton, including carcasses, are increasingly recognized as being quite abundant in the mesopelagic water (Böttger-Schnack, 1996; Roe, 1988; Terazaki and Wada, 1988; Wheeler Jr, 1967). It is impossible to assess whether the damages of the organisms

observed on the digitized organisms were inflicted by the net tow. This is even harder to assess in the deeper nets which spent more time in the water column. Therefore, we cannot tell whether the organisms were damaged during the sampling process or dead beforehand. We attempted to separate the carcasses from the complete bodies of copepods based on grey intensity criteria or by looking at the physical integrity of the organisms, but this was not successful because of independent and continuous changes for both criteria. Nonetheless, among the 110'000 vignettes of copepods, 21'117 (20%) were initially classified as possible carcasses. Their proportion was equal to 42.90% in the surface layer, 26.71% in the upper mesopelagic and 30.39% in the deepest layers. The median and interquartile of abundances varied from the surface (median = 1.21 Ind/m^3, IQR = 2.53) to the upper mesopelagic (median = 0.75, IQR = 0.89) and increased towards deeper layers (median = 0.85, IQR = 0.99). Subsequent data analyses showed that aggregating them or not with the non-damaged copepods had no effect on the analysis' results because their proportion was homogeneous across sampling sites. Therefore, all copepods were ultimately pooled together for all our numerical analyses.

Zooplankton and micronekton perform diel vertical migration (DVM) in all oceans (Banse, 1964). Depending on the organism's taxonomic group and size, ranges of diel migration show tremendous variability (Ohman and Romagnan, 2016; Tarling et al., 2004) . In our study, significant differences in abundances between day and night samples was found for a few groups known to be diel migrators (Euphausiids, Metridinidae, Corycaeidae, Cnidaria for abundance data; and Eumalacostraca and Ostracoda for biomass data). However, at the community level (i.e., total mesozooplankton), no significant differences could be found between the day and night samples at surface. However, total zooplankton biomass was higher in night samples compared to day samples, because of the more abundant large-bodied migrators (Eumalacostraca, Euphausiacea, Table S2). For abundance, this is a rather unexpected result as a large number of zooplankton taxa perform DVM (Kiørboe et al., 2018; Ohman and Romagnan, 2016). Yet, this absence of significant changes had already been observed in previous studies using similar types of plankton nets (Wishner et al., 2018). DVM could not be detected from the ANOSIM analysis of the surface layer for different reasons. First, the weak diel differences in abundances could easily be smeared by plankton patchiness when the replicates are too low. Second, it is possible that no differences were observed because the large organisms carrying out DVM are too few in number compared to the smaller ones in the present data. Day and night differences between the slopes of the total biomass were found, probably due to the few diel migrators species. Hence, it is well known that large zooplankton (euphausiids, sergestid shrimps, amphipods, fish such as myctophids(Morrison et al., 1999))

sampled with larger Multinet nets (opening >1m^2 and mesh size >500µm), or detected through acoustics techniques, showed stronger DVM than smaller organisms collected through smaller Multinet nets such as ours (opening of 0.25 m^2 and mesh size of 300µm). Furthermore, copepods contributed to nearly 80% of total zooplankton abundance in our samples, and copepod DVM may be confined most typically to populations living within the epipelagic zone (Madhupratap et al., 2004; Morrison et al., 1999; Smith et al., 1998).

Many studies have reported midwater peaks of zooplankton and nekton in 100-200 m depth layers centered around 40 to 600 m depth (Andersen et al., 1998; Irigoien et al., 2014; Koppelmann et al., 2004) indicating that the use of a simple power law to describe plankton biomass may be an oversimplification of the true vertical zonation. The general lack of such peaks may be explained by the variability in methods used between studies. Midwater peaks are often reported with instruments allowing a good vertical resolution (> 10 observations in the upper kilometer) and targeting the large migrating organisms with nets having large mesh size or acoustic devices with frequencies adapted to nektonic organisms. Many studies using Multinets equipped with rather fine mesh size (<500µm) do not capture such peaks in abundance/ biomass (Homma and Yamaguchi, 2010; Yamaguchi et al., 2002). In our study, the mesopelagic layer was sampled down to 900 m depth, and only with 2 or 3 nets with a mesh size of 300µm and a small net opening (0.25 m^2). Therefore, midwater peaks could have been smoothed in the few layers. Hence, the power law simplification may be a proper proxy for the smaller fraction of the mesozooplankton (mainly copepods smaller than 2 mm).

Community vertical distribution

On a global scale, zooplankton average abundance and biomass decreased drasctically with depth, with quasi similar patterns for the eight main zooplankton groups (Fig. S1). The strongest variation in abundance was observed for copepods, followed by chaetognaths, small omnivorous zooplankton and crustacean decapods (Fig. S1). The strongest variation in biomass with depth were observed for copepods followed by decapods, chaetognaths and small omnivorous zooplankton (Fig. S2).

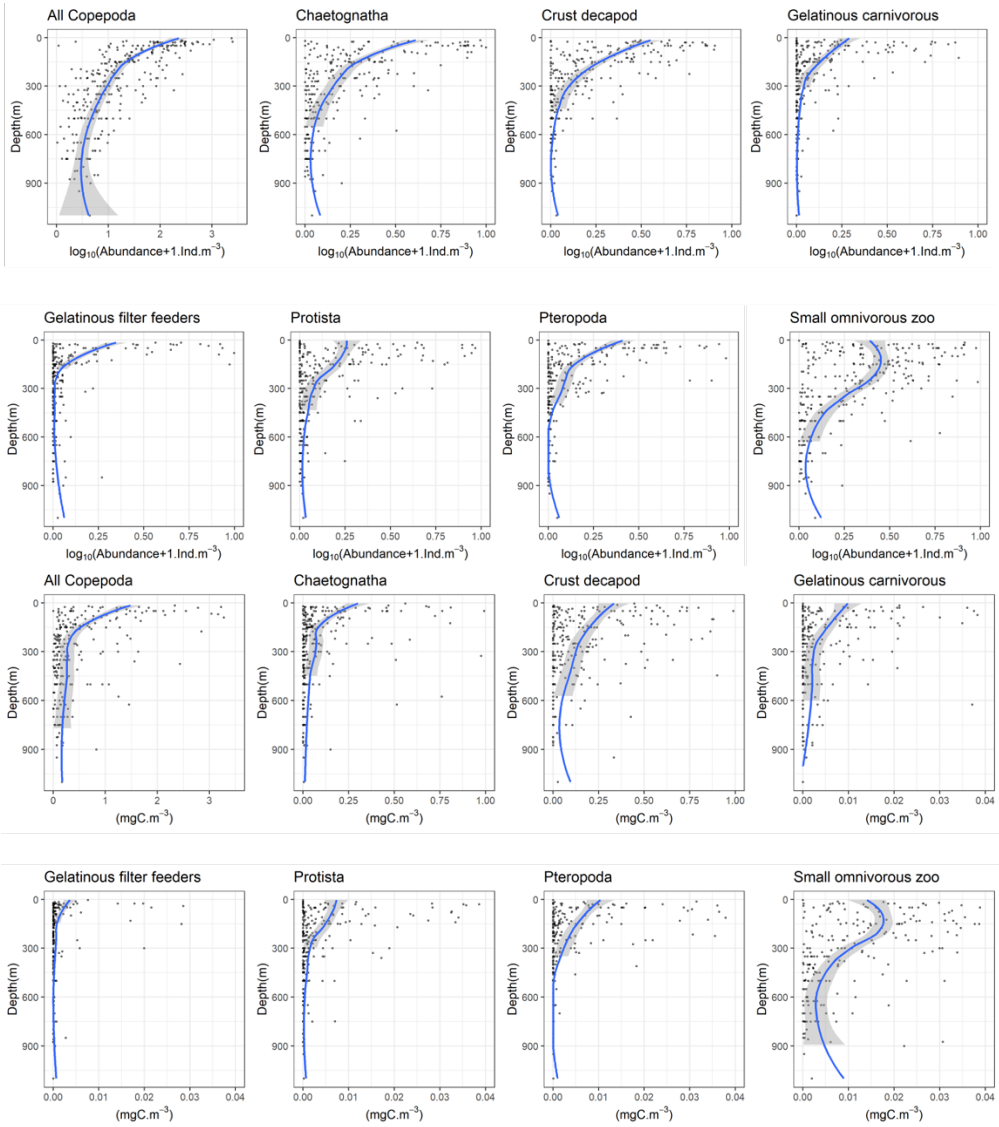

Fig. S1: Vertical profiles of abundance (two first lines) and biomass (two last lines) in the global ocean for the 8 functional mesozooplankton groups: all copepoda, chaetognatha, crustacean decapoda (crust decapod), gelatinous carnivorous, gelatinous filter feeders, protista, pteropoda, small omnivorous zooplankton. Not all abundance and biomass scales are similar to better observe the gradients. In all

cases, solid lines correspond to a smooth trends and gray ribbons to the 95% confidence intervals. These trends are drawn for illustrative purposes and were not used in down- stream analyses.

Community composition in the upper first kilometer of the ocean

When analyzing all vertical layers together, the redundant discriminant analysis (RDA) indicated that environmental variables explained 27.01% of the variance in mesozooplankton groups abundance (Fig. 4). The first RDA axis (RDA1; 47.08% of the variance constrained by the RDA) opposed the samples from polar waters (Arctic Ocean, Southern Ocean; RDA1 > 0) to the samples taken at lower latitudes (Indian Ocean, Northern and Southern Atlantic Ocean, Northern and Southern Pacific Ocean; RDA1 < 0), especially for epipelagic and upper mesopelagic samples. RDA1 was negatively scored by variables depicting a gradient of tropical to extratropical conditions: temperature, salinity, and the relative contribution of picophytoplankton and nanophytoplankton to phytoplankton community biomass. Meanwhile, RDA1 was positively scored by dissolved oxygen concentration, the intensity of the vertical particle flux and its attenuation rate, the concentration of suspended particles and the contribution of microphytoplankton to total phytoplankton biomass. The second RDA axis (22.22 % of the constrained variance) opposed the samples from the surface (RDA2 < 0) to the samples from mesopelagic layers (RDA2 > 0). This axis was positively scored by depth, salinity, and nitrate concentrations, and negatively scored by pico-, nano- and microphytoplankton concentrations, oxygen concentration, particles and chlorophyll *a* concentrations. Samples from the epipelagic layer of higher latitudes showed higher plankton abundances and were dominated by Calanidae and crustacean larvae (copepod nauplii). Samples from the epipelagic layers of lower latitudes Tropical Ocean were more diverse as they displayed more even contributions of Protista, Eumalacostraca, Annelida, Amphipoda, Tunicata, Corycaeidae, Chaetognatha, Euphausiacea, Oithonidae, Cnidaria, Mollusca and Cladocera. In the mesopelagic layer, communities were less spread in the RDA space than for the surface layer. Mesopelagic communities were dominated by Other Copepoda and Metridinidae at higher latitudes and by Calanoida, Ostracoda and Oncaeidae at lower latitudes. Polar and temperate waters displayed lower mesozooplankton diversity but higher mesozooplankton abundances/biomass, more intense vertical particle fluxes, and stronger particle attenuation rates. On the opposite, the warmer and more oligotrophic tropical waters displayed lower diversity, lower mesozooplankton biomass/ abundance, but higher attenuation rates of mesozooplankton organisms. To better disentangle the relationships between

mesozooplankton composition and the environmental conditions within the different vertical layers of the ocean, separate RDAs were then performed for each depth layer.

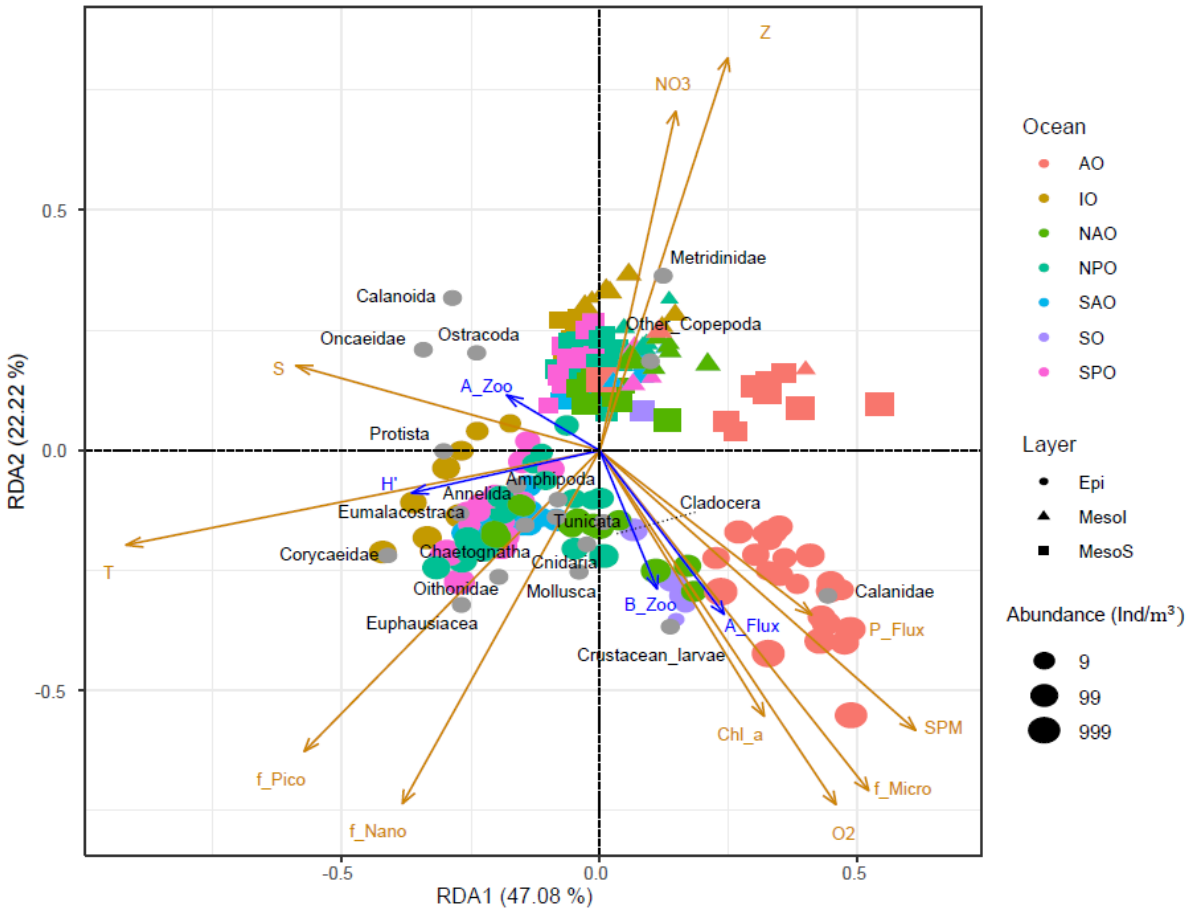

Figure S2: RDA performed with all layers. Each colored dot corresponds to a sample, i.e., one net at one depth at one station. The orange arrows mark the projection of the environmental variables in RDA space: f_pico, f_nano and f_micro correspond to the relative contribution (%) of pico-, nano- and micro-phytoplankton to total phytoplankton biomass, median value of (O2 = dissolved oxygen concentration (µmol/kg), Chl_a = Chlorophyll a concentration (mg/m3), SPM = suspended particles matter (m/sr), T = temperature (°C), Sal = salinity, NO3 = nitrate concentration (mol/L), Z = depth (m)) and P_Flux= particulate flux ($mg.m^{-2}.d^{-1}$)). Grey dots mark the projection of the zooplankton groups abundance ($ind.m^{-3}$). Colors correspond to the ocean basin where the samples were taken: AO = Arctic Ocean, IO = Indian Ocean, NAO = North Atlantic Ocean, NPO = North Pacific Ocean, SAO = South Atlantic Ocean, SO = Southern Ocean, SPO = South Pacific Ocean. Shapes illustrate the vertical layers where the samples were taken: Epi = epipelagic, MesoS = upper mesopelagic and MesoI = lower mesopelagic.

Table S1: List of nets that were removed from the RDA analysis. AO=Arctic Ocean, IO=Indian Ocean, NAO=North Atlantic Ocean, NPO=North Pacific Ocean, SAO=South Atlantic Ocean, SO=Southern Ocean or Austral Ocean, SPO=South Pacific Ocean.

Ocean Bassin	Nets
IO	36_4,38_4, 39_2, 42_3
AO	163_2, 163_3, 206_2
NAO	142_4,142_4n,143_3,143_3n,147_3,147_4,150_1,150_4,151_2,151_4,152_2,152_3,155_2,158_2
NPO	131_2, 132_2,133_3,135_2,137_3,137_3n
SAO	131_2, 132_2,133_3,135_2,137_3,137_3n
SO	84_1, 85_1, 85_2
SP0	98_2, 98_3, 102_1, 106_2, 106_4,109_1,110_1,110_1n,111_1,111_1n,122_1,122_1n,125_1,125_3,127_2,127_2n

Table S2: Wilcoxon test for day and night for each taxon at level of 5% (bold values mean significant test)

	Wilcoxon p-value (abundance)		Wilcoxon p-value (biomass)	
Species	**Epipelagic**	**Upper Mesopelgic**	**Epipelagic**	**Upper Mesopelgic**
Protista	0.50	0.13	0.8	0.06
Annelida	0.66	0.82	0.62	0.57
Chaetognatha	1	0.20	0.58	0.32
Tunicata	0.26	0.078	0.06	0.19
Cnidaria	0.90	**0.037**	0.58	**0.009**
Mollusca	0.95	0.123	0.26	0.96
Eumalacostraca	0.39	0.62	**0.049**	0.49
Euphausiacea	0.21	**0.0098**	**0.0001**	0.63
Amphipoda	0.07	0.91	0.39	0.83
Ostracoda	0.32	0.96	**0.049**	1
Crustacean_larvae	**0.01**	0.81	0.23	0.81
Other_Copepoda	0.76	0.46	0.95	0.41
Calanoida	0.10	0.24	0.11	0.32
Oithonidae	0.19	1	0.24	0.84
Corycaeidae	**0.01**	1	**0.016**	0.76
Oncaeidae	0.66	0.41	0.8	0.51
Metridinidae	**0.0001**	**0.018**	**0.0001**	**0.006**
Calanidae	0.29	0.12	0.07	1

1209